OXFORD

Cerebral Cortex, 2023, **33**, 5163–5180
https://doi.org/10.1093/cercor/bhac407
Advance access publication date 26 October 2022
Original Article

Virtual reality-based sensorimotor adaptation shapes subsequent spontaneous and naturalistic stimulus-driven brain activity

Meytal Wilf[1,2,*], Celine Dupuis[3], Davide Nardo[4,7], Diana Huber[1], Sibilla Sander[1], Joud Al-Kaar[5], Meriem Haroud[1,5], Henri Perrin[1], Eleonora Fornari[6], Sonia Crottaz-Herbette[3,5,†], Andrea Serino[1,3,†]

[1]MySpace Lab, Department of Clinical Neurosciences, Lausanne University Hospital (CHUV) and University of Lausanne, Avenue Pierre Decker 5, 1011 Lausanne, Switzerland,
[2]Center of Advanced Technologies in Rehabilitation (CATR), Sheba Medical Center, Tel Hashomer 52621, Israel,
[3]MindMaze SA, Chemin de Roseneck 5, 1006 Lausanne, Switzerland,
[4]MRC Cognition and Brain Sciences Unit, University of Cambridge, 15 Chaucer Rd, Cambridge CB2 7EF, United Kingdom,
[5]Neuropsychology and Neurorehabilitation Service, Lausanne University Hospital (CHUV) and University of Lausanne, Avenue Pierre Decker 5, 1011 Lausanne, Switzerland,
[6]Biomedical Imaging Center (CIBM), Department of Radiology, Lausanne University Hospital (CHUV) and University of Lausanne, Rue du Bugnon 46, 1011 Lausanne, Switzerland,
[7]Department of Education, University of Roma Tre, Rome, Italy

*Corresponding author: Center of Advanced Technologies in Rehabilitation (CATR), Sheba Medical Center, Tel Hashomer 52621, Israel.
Email: meytalwilf@gmail.com

[†]Sonia Crottaz-Herbette and Andrea Serino contributed equally.

Our everyday life summons numerous novel sensorimotor experiences, to which our brain needs to adapt in order to function properly. However, tracking plasticity of naturalistic behavior and associated brain modulations is challenging. Here, we tackled this question implementing a prism adaptation-like training in virtual reality (VRPA) in combination with functional neuroimaging. Three groups of healthy participants ($N = 45$) underwent VRPA (with a shift either to the left/right side, or with no shift), and performed functional magnetic resonance imaging (fMRI) sessions before and after training. To capture modulations in free-flowing, task-free brain activity, the fMRI sessions included resting-state and free-viewing of naturalistic videos. We found significant decreases in spontaneous functional connectivity between attentional and default mode (DMN)/fronto-parietal networks, only for the adaptation groups, more pronouncedly in the hemisphere contralateral to the induced shift. In addition, VRPA was found to bias visual responses to naturalistic videos: Following rightward adaptation, we found upregulation of visual response in an area in the parieto-occipital sulcus (POS) only in the right hemisphere. Notably, the extent of POS upregulation correlated with the size of the VRPA-induced after-effect measured in behavioral tests. This study demonstrates that a brief VRPA exposure can change large-scale cortical connectivity and correspondingly bias visual responses to naturalistic sensory inputs.

Key words: brain plasticity; fMRI; movie; prism adaptation; resting-state.

Introduction

"No man ever steps in the same river twice, for it is not the same river and he is not the same man" says the ancient Greek statement attributed to Heraclitus. Indeed, our every-day sensory experiences and interactions with the world shape the way we act and perceive. How do these interactions forge our brain? Neuroimaging studies targeted changes in brain activity and connectivity following novel sensory experience. There is ample evidence for experience-induced modulations on resting state connectivity. For example, visual perceptual learning was shown to modulate spontaneous connectivity between the visual and fronto-parietal networks engaged by the task (Lewis et al. 2009). Associative cortical areas and hippocampus increased connectivity following a visual encoding task (both in real life Tambini et al. 2010; and in virtual reality Gauthier et al. 2020). Frontoparietal and cerebellar networks functional connectivity strengthened after exposure to a visuomotor adaptation (Albert et al. 2009). In addition to changes in resting-state connectivity, sensorimotor training was shown to modulate subsequent task-induced activations. For instance, activation in motor regions was upregulated following motor sequence learning (area M1 in Karni et al. 1995; and premotor cortex in Berlot et al. 2020). Visual motion aftereffect was found in area MT following adaptation to a moving stimulus (Tootell et al. 1995), and auditory frequency discrimination training was shown to enhance auditory activation in proportion to performance gain (Jäncke et al. 2001). However, previous studies on experience-induced modulations focused mainly on local effects, restricted to the specific task and brain region being trained. It remains unknown how recent sensory experience affects subsequent visual response to task-free naturalistic stimuli, possibly relying on long-range connections.

Neuropsychological disorders lead to biased sensory representations and aberrant interactions with the environment. Thus, they entail continuously altered sensory experience, which might also permanently affect brain responses. A paradigmatic case is hemispatial neglect syndrome ("neglect"), whereby, usually right

Received: March 9, 2022. **Revised:** September 15, 2022. **Accepted:** September 16, 2022

hemisphere damage causes patients an inability to attend to and interact with stimuli in the left side of space. In many cases, the lesion affects key fronto-parietal regions in the attentional networks (Corbetta and Shulman 2011), while keeping the sensory cortices intact. Nevertheless, the effects of the lesion span well beyond the focal damage, causing a general imbalance of brain activity and connectivity (Baldassarre et al. 2014; Lunven and Bartolomeo 2017; Xu et al. 2019), as manifested also in reduced anticorrelation between attentional networks and the default mode network (DMN; Baldassarre et al. 2014; Siegel et al. 2016). These recent findings emphasize the role of fronto-parietal attentional and DMN regions in mediating representation and processing of multisensory inputs for well-functioning sensorimotor interactions.

In the current study, we implement a novel virtual reality-based visuomotor adaptation training to affect the way healthy people interact with and represent the environment. We ask whether and how such training, which induces a shift of reference frames, modifies large scale brain network connectivity and the processing of naturalistic stimuli. To this aim, we base on a prominent method for studying visuomotor plasticity in healthy individuals, as well as for rehabilitating neglect patients, called prism adaptation ("PA"). It consists of performing repetitive goal-directed movements while wearing prismatic lenses that induce a lateral shift of visual inputs, resulting in well-established sensorimotor aftereffects, for instance spatial biases in open-loop reaching tests after prism removal ("PA aftereffects"; cf. Redding and Wallace 1996). PA aftereffects span well beyond the motor domain, affecting various attentional and perceptual tasks, in both neglect patients and in healthy individuals (Jacquin-Courtois et al. 2013; Michel 2015), and persisting long after the adaptation training had ended (> 40 min) (Schintu et al. 2014). PA aftereffects were shown to manifest also in brain activity, as changes in activation of the inferior-parietal lobule (IPL) during visual attention task (Crottaz-Herbette et al. 2014, 2017b), and modulations of task-free resting-state connectivity (Schintu et al. 2019; Tsujimoto et al. 2019; Wilf et al. 2019; Gudmundsson et al. 2020; see Panico et al. 2020 for review).

These previous studies largely used artificial, non-ecological setups while testing for PA-related aftereffects in functional magnetic resonance imaging (fMRI). We propose that in order to gain better understanding of real-life-like aftereffects of sensorimotor adaptation, the fMRI paradigms testing its brain effects should adopt a naturalistic approach (cf. recent opinion by Nastase et al. 2020). Thus, in order to enhance the ecological nature of the adaptation training while keeping well-controlled environment, we here implement PA-like sensorimotor adaptation training in an immersive VR environment (VRPA) embedding dynamic visual targets and a gamified activity. In three different groups of participants, we introduced a rightward, a leftward, or a sham visuomotor rotation, and assessed the related behavioral spatial biases (see Fig. 1a and b). To characterize the mechanisms underlying short-term VR experience-induced modulations in free-flowing brain activity, we investigated VRPA-induced changes in cortical functional connectivity patterns, changes in activation pattern in response to naturalistic stimuli, and their link with well-known PA behavioral aftereffects (see Fig. 1).

Materials and methods

Participants

The study comprised 45 healthy young adults, which were divided into 3 independent groups of participants: A first group of 16 participants performed rightward adaptation training (aged 23 ± 3; 8 females), a second group of 14 participants performed sham training (aged 24 ± 4; 7 females), and a third group of 15 participants performed leftward adaptation training (aged 23 ± 4; 8 females). Required sample size was estimated based on our previous study that measured resting state modulations following standard PA (Wilf et al. 2019). All participants were right-handed with normal or corrected-to-normal vision and no neurological or psychiatric pathologies. Participants gave written informed consent according to procedures approved by the local Ethics Committee (CER-VD protocol no. 2017-01588). All participants were naïve regarding the aim of the study, and had no prior visuomotor adaptation experience.

Procedures

Experimental session overview

An experimental session lasted ~120 min, and included 2 phases of VR training interleaved with 2 identical phases of fMRI (pre–post adaptation; see Fig. 1): A session started with a "baseline VR phase" in which participants from all 3 groups had to hit dynamic targets with a virtual hand without any spatial shift. This was followed by a series of standard adaptation "aftereffect tasks" aimed at revealing proprioceptive-motor spatial biases (including pointing straight ahead with eyes closed). This was followed by "pre-adaptation fMRI sessions" assessing task-free brain activity, namely, "resting state" and free-viewing of "naturalistic stimuli" (Fig. 1b and c). The left VRPA group had a different fMRI paradigm from which we analyzed only the resting-state runs. This group did not watch the naturalistic videos, which were available only for the right- and sham-VRPA groups. The initial paradigm of the left VRPA group included other visual stimuli (a replay of a VRPA training session). As these stimuli induced excessive drowsiness, the data could not be used. Consequently, this protocol was not applied to the right VRPA group nor the sham group (whose data were collected afterward), for which we used the more effective naturalistic visual paradigm presented here, which indeed showed a better compliance rate. Participants then performed the "VRPA session" outside the MRI, with either left/right/sham shift between their real hand and the virtual hand. This was followed by "behavioral aftereffect tasks." Immediately afterward, participants went back in the MRI for the "post-adaptation phase" and performed an identical experimental sequence including "resting-state" and "naturalistic videos." Lastly, participants repeated the "pointing straight ahead" task outside the scanner at the end of the experiment.

Virtual reality device and setup

During the virtual reality training and tests, participants were seated on a chair in a fixed position, whereas the experiment was presented via a head mounted dievice (HMD; "Oculus Rift" consumer version 1, 1,080 × 1,200 resolution per eye, 110° field of view, refresh rate of 90 Hz). Participants were immersed in a unique 3D VR environment depicting a tennis field, which was developed using Unity Software (consumer version 2019.2.13), and used their right hand to control a virtual hand in the virtual world (see Fig. 1a; Oculus Touch by Oculus).

The sequence of tasks was as follows (see Fig. 1b):

Baseline VR phase

At the beginning of the experiment, participants performed 60 trials of baseline VR training outside the MRI without any visuomotor shift, during which they had to use the virtual hand to catch tennis balls that were thrown at them from the other side of the tennis field (see section "VRPA training" for details).

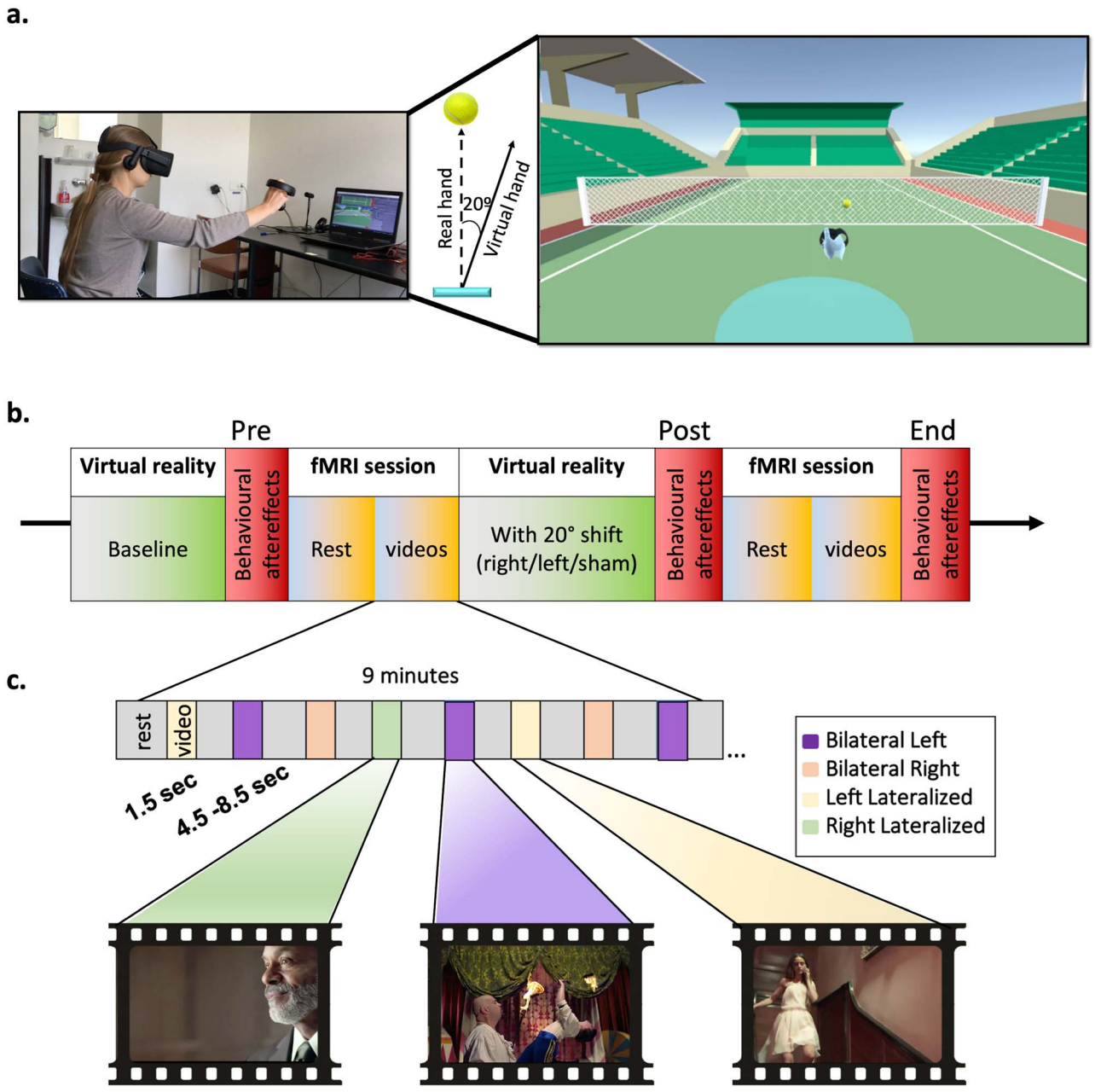

Fig. 1. Experimental paradigm and procedure. a) Schematic representation of virtual reality prism adaptation (VRPA) training. Participants were immersed in a 3D virtual environment and had to catch dynamic targets (tennis balls) using a virtual hand. During adaptation sessions, a 20° rightward/leftward angular shift was introduced between the participants' real hand and the virtual hand. b) Experimental procedure. The session always began with baseline VR training with no shift, followed by behavioral tests for assessing proprioceptive-motor spatial biases, including manual pointing straight ahead with eyes closed. Afterwards, participants underwent resting-state fMRI and a free viewing of a sequence of naturalistic videos. They then performed VRPA outside the scanner, with either right ($n = 16$), Left ($n = 15$); or no shift ($n = 14$), followed by an identical set of behavioral tests and fMRI tasks. At the end of the session, behavioral aftereffects were again measured outside the scanner. c) Scheme of naturalistic videos task. Videos lasted 1.5 s and contained a salient stimulus on either the right/left side of the screen, or on both sides of the screen, with the more salient stimulus on the right/left side (20 videos in each category; videos taken from Nardo et al. 2016; Nardo et al. 2019).

Behavioral aftereffect tasks

Immediately following the baseline VRPA training (without shift), participants performed several behavioral tasks meant for assessing their proprioceptive-motor spatial biases prior to adaptation. These tasks included reaching straight ahead with eyes closed, open-loop pointing to visual targets on the left and right side in VR (without feedback regarding hand position), open-loop pointing to visual targets outside VR (standard PA aftereffect procedure), and line bisection tasks on pen & paper. Because of its relative reliability in capturing purely proprioceptive-motor aftereffects devoid of visual cues or credit attribution bias to the VR system confounds (Fleury et al. 2019), only the pointing straight ahead task will be presented in the scope of the current paper.

Pre-VRPA fMRI phase

The fMRI session started with an 8-min run of resting state with eyes closed, followed by a 7-min run of visual attention task (not covered in this paper), and a 9-min naturalistic stimulus run,

in which participants freely viewed a series of short videoclips portraying everyday life scenes (videos taken from Nardo et al. 2016, 2019; see Fig. 1c).

VRPA phase

Participants went out of the MRI for an additional VR training phase, this time performing 160 trials of the tennis game with a 20° rotational shift between the virtual and their real hand, namely visuomotor adaptation (see section "VRPA training" for details; no shift was introduced for the sham group), followed by identical aftereffect tests to probe adaptation-induced behavioral aftereffects.

Post-VR-adaptation fMRI phase

Immediately following the VR session, participants went back in the MRI (they had to cross their hands and were not allowed to use them during the transition in order to avoid potential de-adaptation). Participants repeated the same fMRI experimental sequence as in the first fMRI session—i.e. rest with eyes closed, visual attention task, and naturalistic viewing task.

Final aftereffect tests

Additional repetition of a subset of the aftereffect tests was performed after the second fMRI phase, to assess the residual behavioral aftereffects also at the end of the fMRI session, i.e. ~40 min past the adaptation phase.

VRPA training

During the VR training phases, participants were immersed in a VR environment of a tennis-field using a natural-looking virtual hand, and were instructed to catch tennis balls that were thrown at them from the far end of the field. Each trial began when participants placed their hand in the "origin position" located a few centimeters in front of the midline of their body, at position [0, 0] on the XZ plane of the virtual environment. To guide participants back to the correct origin position, the area around it was marked by a semi-transparent turquoise semicircle (30-cm radius). The following trial was launched only when participant's hand was placed back in the origin position. Importantly, the participants' virtual hand was invisible while the hand was within the radius of the round table (~30 cm from the origin position), and became visible only in the last segment of the reaching movement trajectory, namely when the hand was already close to the target. This partial visual feedback of hand trajectory enables both strategic and online mechanisms to take place during adaptation (Facchin et al. 2020; Wilf et al. 2021). In each trial, the tennis ball approached the participant at a constant speed randomly selected within the range of comfortable ball speeds. The balls were thrown from 1 of 4 initial positions—either the far left position/the far right position, above/below participant's arm height (initial positions ranged from −2 to 2 m on the x axis, and 0.2 to 1.8 m on the y axis, equidistant 4 m from the origin position), and moved towards 1 of 24 possible terminal positions equally spread around the midline, resulting in an equal number of balls moving from left to left, left to right, right to right, and right to left hemifields (Fig. 1a; terminal positions ranged from −0.4 to 0.4 m on the x axis, and from 1 m to 1.2 m on the y axis, equidistant 0.45 m from the origin position). The order of trials was randomized in each session. When catching the ball, participants received multisensory positive feedback: a wind-chime auditory sound, a light vibration tactile feedback of the controller, and a bright glitter visual effect. Participants were able to catch the balls also before or after they reached the intended terminal positions, but in case a ball was not caught, it either continued to move and disappeared behind the participant, or it "blew up" before it reached the turquois area surrounding the participant. The radius for catching the targets was limited to a minimum of 30 cm in order to force the participants to perform large and quick reaching movements that enable proper adaptation, and to prevent the ball from arriving too close to the participant's body.

During the VRPA session, a rightward/leftward 20° rotational shift was induced between the real hand and the virtual hand (see Fig. 1a) on the 11th trial (similarly to Wilf et al. 2021). During baseline and sham-VRPA sessions, the virtual hand and the real hand were always aligned.

Straight ahead pointing task

Participants were instructed to close their eyes and reach straight ahead in front of the midline of their body. Once they reached their subjective midline position, they pressed the trigger button of the VR controller with their index finger, and returned their hand to the origin position near their body. The pointing error was calculated as the angular deviation from the true midline (referred to as 0 on the x axis, directly in front of the origin position). This procedure was repeated 5 times, and the 5 movements were averaged to establish the participant's pointing error in each of the phases of the experiment (see Fig. 1b): pre (immediately following the VR-baseline session), post (immediately following the VRPA session), and end (following the second fMRI session, ~40 min following adaptation).

An additional open loop aftereffect test was performed outside the VR environment, where participants had to look at either left or right targets and then reach them with their eyes closed (see Crottaz-Herbette et al. 2014 for standard open loop test procedure). The angular target error at each experimental phase was calculated as in the pointing straight ahead task.

A 2-way repeated measures analysis of variance (ANOVA) was performed for each of the aftereffect tests separately using the JASP software version 0.11.1, with within-subject factor phase (pre/post/end) and between subjects factor group (right-VRPA/left-VRPA/sham-VRPA), followed by post-hoc tests.

Imaging setup and fMRI data analysis

MRI data of right-VRPA and sham-VRPA groups was collected with a 3T Siemens Magnetom Prisma scanner with a 64-channel head-coil, located at the Lemanic Biomedical Imaging Center (CIBM), and data of group left-VRPA was collected at the Laboratory for Research in Neuroimaging (LREN) in the Centre Hospitalier Universitaire Vaudois (CHUV), Lausanne. Functional MR images were acquired with a multiband-2 echo planar imaging gradient echo sequence (repetition time 2 s; flip angle 90°; echo time 30 ms; number of slices 66; voxel size 2 × 2 × 2.04 mm; 10% gap). The 66 slices were acquired in a sequential ascending order and covered the whole head volume in the AC–PC plane. A high-resolution T1-weighted 3D gradient-echo sequence was acquired for each participant (right VRPA group: MP2RAGE as described in (Marques et al. 2010); sham and left VRPA groups: MPRAGE, voxel size 1 × 1 × 1 mm). To prevent head movements in the coil, padding was placed around the participant's head.

Task 1: fMRI data analysis resting state data

MRI data preprocessing

Data were processed using FSL 5.0.10 (www.fmrib.ox.ac.uk/fsl) and in-house Matlab code (Mathworks, Natick, MA, United States). Functional data of all groups was analyzed with an identical

pipeline, whereas for right VRPA group, because of the use of MP2RAGE, an additional step was taken in the analysis of the anatomical scans in order to unite the sparse MP2RAGE images into a single anatomical file (brightness threshold 90, and multiply INV2 and UNI for noise removal; Marques et al. 2010).

Functional data were analyzed using FMRIB's expert analysis tool (FEAT, version 6). The following pre-statistics processing was applied to the data of each participant: motion correction using FMRIB's Linear Image Registration Tool (MCFLIRT); brain extraction using BET. For right VRPA group, the BET was performed on the INV2 contrast file for better brain extraction (Choi et al. 2019); high-pass temporal filtering with a cut-off frequency of 0.01 Hz; removal of the first 2 volumes from each functional run, and 5-mm Gaussian spatial smoothing. Functional images were aligned with high-resolution anatomical volumes initially using linear registration (FLIRT), and then optimized using boundary-based registration. Structural images were then transformed into standard MNI space using nonlinear registration tool (FNIRT), and the resulting warp parameters were applied to the functional images as well. All the functional images were resampled to $2 \times 2 \times 2$ mm^3 standard space, and therefore all further analyses were performed in standard MNI space.

Only for resting-state data, additional denoising steps were performed: A scrubbing procedure was applied for censoring motion-contaminated frames using the framewise displacement (FD) and the DVARS measures (Power et al. 2014). Then regressing out of signals from the white matter and ventricles was performed as follows: The white matter and ventricles of each participant were automatically defined using FSL's FAST (Zhang et al. 2001), and eroded to avoid boundaries between tissues (Hahamy et al. 2014). The non-neuronal contributions to the blood oxygen level-dependent signal were removed by linear regression of motion parameters, ventricle and white matter timecourses for each participant (Fox et al. 2009), whereas no global signal regression was performed (Weissenbacher et al. 2009; Hahamy et al. 2014; Murphy and Fox 2017). Two participants from the right VRPA group were removed from analysis because of prolonged contamination by excessive head motion (> 4 mm), resulting in 14 participants for the resting state right-VRPA group, 15 participants for the left-VRPA group, and 14 participants for the resting state sham group.

Atlas-based segmentation and network labeling

Cortical regions of interest (ROIs) for resting-state connectivity analysis were defined based on the Harvard-Oxford (H-O) probabilistic atlas (as implemented in FSL software; Desikan et al. 2006). In order to obtain a single H-O ROI label for each voxel, a "winner take all" approach was applied, by which each voxel receives the label of the ROI with the highest probability. This was implemented through the use of the atlas-labeled map in FSL (as presented also in Fig. 3a). The definition of regions was performed for each participant as following: First, the atlas label mask was multiplied by the individual subject's gray matter mask (as defined by FSL's FAST) to exclude voxels outside the brain. Then, to enable comparison between left and right hemispheres, the 48 atlas-defined regions were each separated to 2 distinct regions in the left and right hemisphere according to *x*-coordinates of the voxels comprising each region, resulting in 48 pairs of homologue regions symmetrical across the 2 hemispheres (see Fig. 3a). In order to sort the regions in a functionally-relevant manner, each region was assigned to 1 of 7 primary functional connectivity resting state networks based on the maximum overlap of the region with the network MNI cortical parcellation (Yeo et al. 2011): visual, somatomotor, dorsal attention network (DAN), ventral attention network (VAN), limbic system, frontoparietal network (FPN), and DMN. The Yeo7 network segmentation was chosen, since it is well accepted and largely captures the networks relevant for visuomotor tasks such as the one used in the current study. Within each network, regions were sorted according to functional subsystems, and arranged from posterior to anterior and from dorsal to ventral (see Fig. 3a and Supplementary Table 1 for full sorted list of regions).

Functional connectivity matrices

A connectivity matrix was calculated for each resting state run for each participant as follows: The mean timecourse of each region was extracted, and pairwise Pearson correlation was calculated for each pair out of the atlas regions, resulting in a 96 × 96 correlation matrix (48 left hemisphere and 48 right hemisphere regions). The order of regions in the matrix remained identical in the left and right hemisphere regions. This resulted in a symmetrical matrix, with upper left quadrant depicting within-hemisphere connectivity in the left hemisphere ("LL"), lower right quadrant depicting within-hemisphere connectivity in the right hemisphere ("RR"), and lower left quadrant depicting connectivity between left and right hemisphere ("LR," the quadrant diagonal represents homotopic connectivity between homologue regions of the 2 hemispheres; see scheme in Fig. 4c).

The single-subject connectivity matrices were Fisher z-transformed and averaged to generate the mean "pre" and "post" resting state connectivity matrices. Each individual participant's "post" and "pre" matrices were subtracted, and the modulation matrices were averaged to visualize the average difference in connectivity between "pre" and "post."

Gaussian mixture model analysis

For assessing the overall distribution of correlation coefficients of the "pre" and "post" single-subject connectivity matrices, a Gaussian mixture modeling approach was implemented (Tyszka et al. 2014). First, to avoid redundancy, only the values below the main diagonal were taken for further analysis (see scheme in Fig. 4c). Then the distribution of correlation coefficients in each matrix was plotted, and fitted with a combination of 2 Gaussian components (see example in Fig. 4a; as implemented in Matlab Statistical Toolbox with 3,000 iterations and 100 replications). Then for each matrix the μ (mean of the Gaussian) accounting for the highest proportion of the data variability was taken as the representative value of the matrix distribution, resulting in 2 μ values for each subject that were taken for further statistical analysis ("pre" and "post"). A 2-way mixed-effect repeated-measures ANOVA (rmANOVA) was then performed using JASP with factors "phase" (pre/post; within-subject factor) and group (right-VRPA/left-VRPA/sham-VRPA; between-subject factor).

To quantify the change in connectivity within each hemisphere and between hemispheres, an analysis based on the same principle was performed separately for each quadrant of the whole connectivity matrix, but this time plotting the distribution of the "difference" matrices (post–pre). The matrices were divided to 3 quadrants—i.e. correlation values depicting left–left connections (LL), right–right connections (RR), and interhemispheric left–right connections (RL; see Fig. 4c; right). Each Gaussian fit was performed separately for each quadrant, resulting in 3-μ values for each subject denoting the difference between "pre" and "post" (for LL, RR, and RL). For the LL and RR submatrices, only values below the diagonal were considered, but since the interhemispheric submatrix RL is not entirely symmetrical, all its values were included in the distribution and not only values below

the subdiagonal (note that homotopic connections along the submatrix diagonal were also included, since they are not equal to 1 and therefore not necessarily cancel out when subtracting "pre" and "post" matrices). The resulting μ parameters were taken to statistical analysis of a 2-way mixed-effect rmANOVA with factors "quadrant" (LL/RR/RL; within-subject) and group (left-VRPA/right-VRPA/sham-VRPA; between-subject).

Task 2: free viewing of naturalistic videos

Design and stimuli

During the pre- and post-fMRI sessions, participants were presented with visual-only videos portraying everyday life scenes without any linguistic content (see Fig. 1c for a few screen shot examples; see Nardo et al. 2016 for more elaborate description of the videos), and were instructed to freely view the videos without any explicit task. We used a well-validated set of videos (Nardo et al. 2016, 2019) showing everyday life situations obtained by editing a collection of TV commercial clips, partly purchased from an Advertising Archive (http://www.coloribus.com) and partly downloaded from YouTube. Stimuli were made up of 1.5-s video-segments that included a single continuous scene with either one lateralized distinctive event (Llat/Rlat) or multiple events in both hemifields (Lbil/Rbil). Most of the distinctive, semantically-relevant events consisted in one or more persons in the foreground, who either performed an action (walking, dancing, manipulating objects, etc.) or changed posture. In ∼10% of videos, the event consisted in a moving vehicle (plane, car, motorbike, etc.; equally distributed across conditions). Stimuli were visual only, containing neither sounds nor any linguistic content. We also discarded any segments that included writings, which allowed us to left–right flip the videos as an additional experimental control. Out of the original stimulus set, 80 videos were selected, divided into groups of 20 videos from 4 different categories according to previously established saliency maps (Nardo et al. 2016): left-lateralized, right-lateralized, bilateral left salient, and bilateral right salient; see Fig. 1c), while ensuring a balanced distribution of objects representing different visual categories (faces, cars, body-parts etc.). Each run began with one 3-s video of visual moving texture, to eliminate the transient response to a novel visual stimulation, which might artificially increase the response to the first trial. The order of videos was pseudorandomized and videos were interleaved with periods of fixation lasting between 4.5 and 8.5 s (event timings were determined using "optseq" tool (Dale et al. 1999). The content of left-salient and right-salient videos was counterbalanced by presenting a horizontally-flipped version of the videos to half of the participants (however, note that each participant viewed an identical version of the videos in the pre- and post-sessions).

MRI data preprocessing

Preprocessing was similar to the one described in section "MRI data preprocessing" for resting state data, with the exception that projecting out and scrubbing were not perform on task-based data, but instead noise factors were controlled through the event-based model. One participant from the right VRPA group was removed from analysis because of prolonged contamination by excessive head motion (> 4 mm), resulting in 15 participants for the videos right-VRPA group, and 14 participants for the videos sham-VRPA group.

Multisubject general linear model analysis

To create task-based statistical parametric maps, a whole brain general linear model (GLM) analysis was applied for each subject using FEAT, modeling each video category with a corresponding regressor (convolved with double-gamma hemodynamic response function). The 6 motion parameters and their derivatives were used as nuisance regressors. In addition, motion-contaminated timepoints were modeled as nuisance regressors using motion outlier detection algorithm implemented in FSL.

This analysis yielded 5 statistical maps of interest: response to all videos, to left-lateralized videos, right-lateralized videos, left-salient bilateral videos, and right-salient bilateral videos. Since each participant underwent 2 identical runs of video presentation, the single-subject analysis resulted in 2 maps for each participant in each condition ("pre" and "post"). A group analysis of "pre" session and "post" session separately was carried out using FMRIB's local analysis of mixed effects (FLAME1). Z statistic images were thresholded using clusters determined by $Z > 2.6$, and a family-wise-error (FWER) corrected cluster significance threshold of $P < 0.05$ was applied to the suprathreshold clusters.

To compare between "pre" and "post" sessions, a within-subject analysis of statistical maps was carried out using a paired 2-group difference design in FMRIB's Mixed Effect Ordinary Least Squares Estimation, cluster thresholded $Z > 2.3$ and $P < 0.05$ (results were verified and replicated also using FSL FLAME1 cluster thresholded $Z > 2.3$ and $P < 0.05$, and SPM paired t-test GLM with threshold 0.005 FDR correction; Supplementary Fig. 4, see online supplementary material for a color version of this figure).

Each of the 4 experimental conditions was examined separately (left/right/unilateral/bilateral videos), as well as joined together to see general responses to naturalistic videos regardless of their spatial layout ("all videos").

Correlation between brain and behavior

The change in cortical activity during movie presentation ("all videos" condition) was tested for an association with the change in pointing straight ahead biases in our group of participants. To that end, a region of interest (ROI) was defined according to the group map generated by contrasting "pre" and "post" responses to all videos (separately for the right VR-adaptation group and for the sham group). The beta value of this ROI from each individual participant was extracted in the "pre" and "post" runs. Then the difference in beta value ("post"–"pre") was compared to the difference in straight ahead pointing error (deviation from true midline) by means of Pearson correlation using JASP software for statistical analysis.

Psychophysiological interaction analysis

Psychophysiological interaction (PPI) analysis was carried out using FSL FEAT, to probe possible interactions between the selected ROI and the rest of the brain, related to videos presentation (right POS ROI was taken for right-VRPA group, bilateral IPS ROI for sham-VRPA group). To that end, the activity timecourse of the ROI was extracted in each participant and each run ("pre" and "post"), and its interaction with an "all videos" regressor was assessed. Then a group GLM analysis was performed on the "pre" and "post" sessions with FLAME1 ($Z > 2.3$, FWER $P < 0.05$ cluster correction).

Results

Behavioral VRPA aftereffects

First, we assessed the behavioral aftereffects induced by the VRPA training. Participants exhibited consistent lateral biases in manual straight ahead pointing with eyes closed following either right

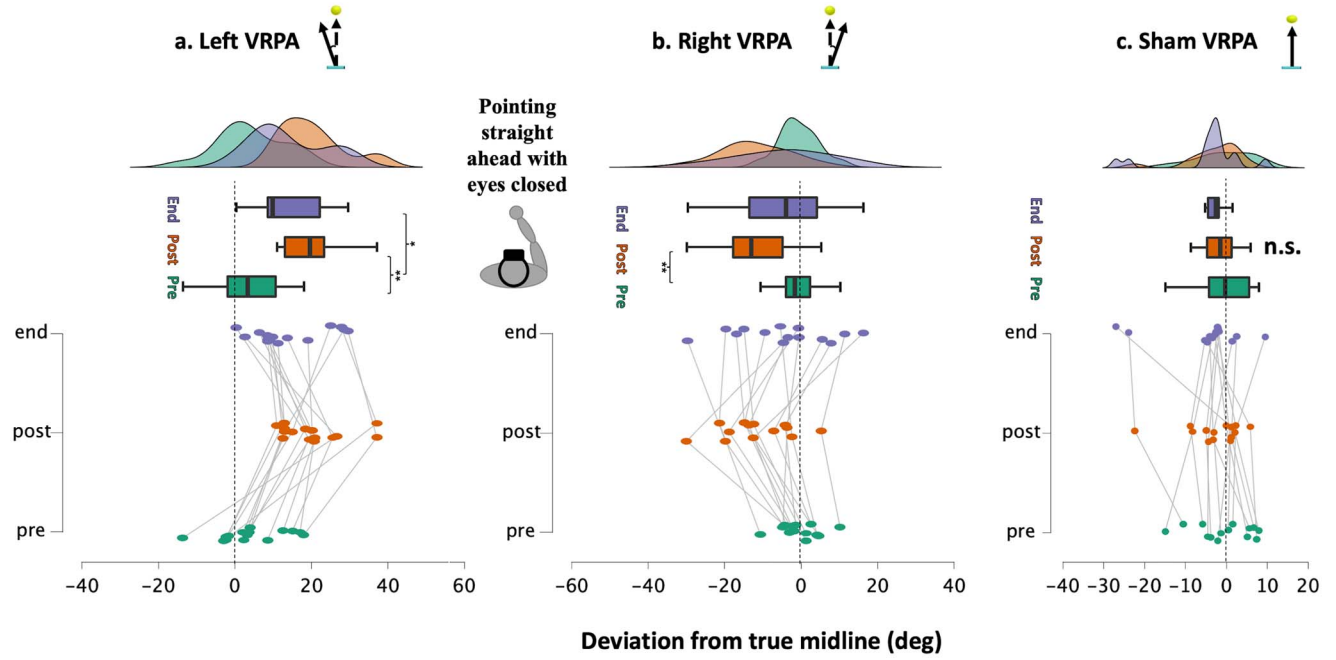

Fig. 2. Behavioral aftereffects following rightward, leftward, and sham VRPA. Participants had to point straight ahead with eyes closed on 3 timepoints during the experimental session: after baseline VR practice ("Pre"), after VRPA training ("Post"), and at the end of the experiment after the fMRI session ("End," ~40 min following adaptation). Raincloud plots show the pointing errors in each group a) left VRPA ($N = 15$), b) right VRPA ($N = 16$), and c) sham VRPA ($N = 14$). Positive values denote rightward deviations, and negative values denote leftwards deviation. * $P < 0.05$; ** $P < 0.001$.

or left VRPA training, but not following sham VRPA, thus demonstrating a clear aftereffect due to the sensorimotor adaptation. Indeed, a 2-way ANOVA with factors group (right/left/sham VRPA) and phase (pre/post/end) revealed an interaction between group an phase ($F(4,80) = 15.9$; $P < 0.001$; see Supplementary Table 2 for detailed post-hoc statistics between the different conditions). Therefore we continued to testing the phase effect in each group separately: In the leftward VRPA group, aftereffect manifested in systematic rightward deviation in pointing straight ahead movements (Fig. 2a; main effect of experimental phase: $F(2,28) = 16.4$; $P < 0.001$), whereas the rightward VRPA group presented leftward deviations following adaptation (Fig. 2b; main effect of experimental phase: $F(2,30) = 13.5$; $P < 0.001$). No systematic pointing error was induced by the Sham VRPA (Fig. 2c; $F(2,26) = 1.9$; $P > 0.15$). Importantly, a residual pointing bias was still evident in both adaptation groups (though nonsignificant in the right-VRPA group) even at the end of the experimental session, i.e. ~40 min after VRPA (Fig. 2a and b; purple; in line with Schintu et al. 2014). These behavioral results validate that the spatial realignment induced by the VRPA training was effective when participants were undergoing subsequent fMRI experiments and that some of the effect remained throughout the entire "post" fMRI session.

VRPA effects on resting-state connectivity

After we established the presence of behavioral aftereffects, we aimed to unravel VRPA-induced modulations in spontaneous, resting-state connectivity. To obtain a complete, unbiased, view of cortical connectivity, we represented the resting-state connectivity pattern as a matrix of correlations between a set of 48 atlas-based cortical ROIs, homologous between the left and right hemispheres, which were sorted according to 7 primary functional networks (see Methods and Fig. 3a). All 3 groups showed typical resting-state connectivity patterns at baseline, prior to VRPA or sham training (Fig. 3b; the right VRPA group showed overall higher baseline connectivity, probably due to interindividual differences). However, when assessing the modulations in connectivity between pre- and post-VRPA, there was a substantial difference between the adaptation groups and the sham group: The left and right VRPA groups showed widespread decreases in connectivity (Fig. 3c; left + middle), whereas the sham group showed only slight increases in connectivity, mainly between visual and motor ROIs (Fig. 3c; right). A qualitative inspection of the modulation matrices revealed that the connectivity decrease in the VRPA groups was most prominent in the connections between the DMN/fronto-parietal networks (FPN) regions, and the 2 main attentional networks—the dorsal and ventral attentional networks (DAN/VAN), including the IFG and STS regions (Fig. 3c; left + middle; black square outlines). Interestingly, whereas following right-VRPA the most pronounced connectivity decreases were evident within the left hemisphere and between left and right hemispheres (Fig. 3c; middle), following left-VRPA the effect was more evident in the right hemisphere and between hemispheres (Fig. 3c; left). Together, these results suggest that VRPA (but not sham VRPA) increases decoupling between DMN/FPN and attentional networks, with more pronounced modulation between hemispheres and within the hemisphere corresponding to the direction contralateral to the induced spatial shift (i.e. right hemisphere for left VRPA and left hemisphere for right VRPA).

In order to quantify the VRPA-induced modulations in resting-state connectivity, we fitted a Gaussian Mixture Model to the distribution of correlation values in each connectivity matrix (see Methods). First, to compare the overall changes in connectivity, the means (μ values) of the fitted gaussians were compared between "pre" and "post" matrices in all 3 experimental groups (see Fig. 4a for 2 single-subject examples of gaussian fitting and mean value extraction). A 2-way mixed-effects ANOVA with factors group (left/right/sham VRPA) and phase (pre/post) revealed a main effect of group ($F(2,40) = 4.54$; $P = 0.017$) and an interaction between group and phase ($F(2,40) = 5.54$; $P = 0.007$). These results

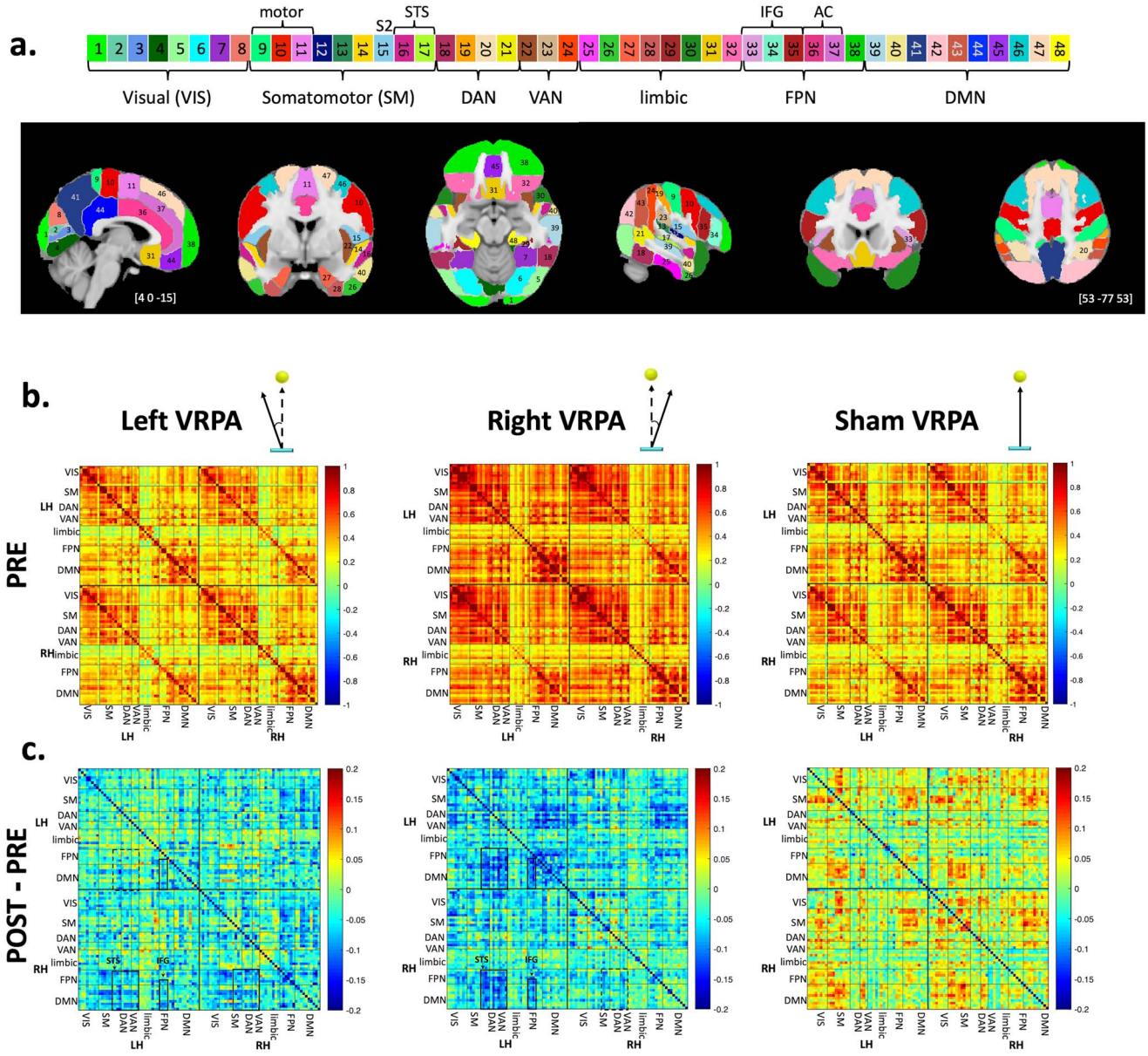

Fig. 3. Resting-state connectivity modulations following VRPA. a) Atlas-based cortical segmentation of MNI brain with network labelling. Color-coded Harvard-Oxford atlas regions are symmetrical across the 2 hemispheres. The atlas regions are labeled and principally sorted according to the 7 primary functional connectivity networks suggested in Yeo et al. (2011), and within each network according to functional subsystems (see methods). b) Mean baseline (pre-VRPA) pairwise functional connectivity matrices between atlas regions in the left and right hemispheres ($N = 14$ for right/sham groups; $N = 15$ for left group). Values are sorted within each hemisphere as denoted in panel a, with identical sorting for left and right hemispheres. Each quadrant represents either within hemisphere connections (LH–LH/RH–RH), or inter-hemisphere connections (RH–LH). c) Mean pairwise connectivity modulations following VRPA (either left/right/sham VRPA groups). Blue colors denote decrease in correlations and warm colors denote increase in correlations. Note that following either type of VRPA (but not sham), there was an overall decrease in connectivity. Black squares highlight clusters of connectivity modulations between DMN/FPN and attentional networks. Homologous connections were modulated across quadrants in the left/right VRPA groups, but with different hemispheric dominance. VIS = visual network; SM = sensorimotor network; DAN = dorsal attention network; VAN = ventral attention network; FPN = frontoparietal network; DMN = default mode network; IFG = inferior frontal gyrus; AC = anterior cingulate; STS = superior temporal sulcus; LH = left hemisphere; RH = right hemisphere.

demonstrate that the pattern of connectivity before and after VRPA varied across the groups.

Next, in order to deeply investigate connectivity changes induced by the different types of visuomotor adaptation, we zoomed in on 3 subtypes of connectivity modulations—within left hemisphere ("LL"), within right hemisphere ("RR") and between hemispheres ("RL"), as represented in different quadrants of the connectivity matrix (see Fig. 4c; right). Specifically, since we aimed to quantify the size of connectivity *modulation* within each quadrant, this time we applied the gaussian mixture model analysis on *the difference matrices* instead of separately for the pre and the post phase (i.e. post–pre matrices; cf. Fig. 3c). We first plotted the distribution of the mean modulation matrices in each quadrant (Fig. 4b), which again revealed a differentiation in the direction of modulation between the sham and the adaptation groups, with a slightly more negative distribution for right VRPA group in the LL quadrant and for the left VRPA in the RR quadrant. To quantify potential differences between

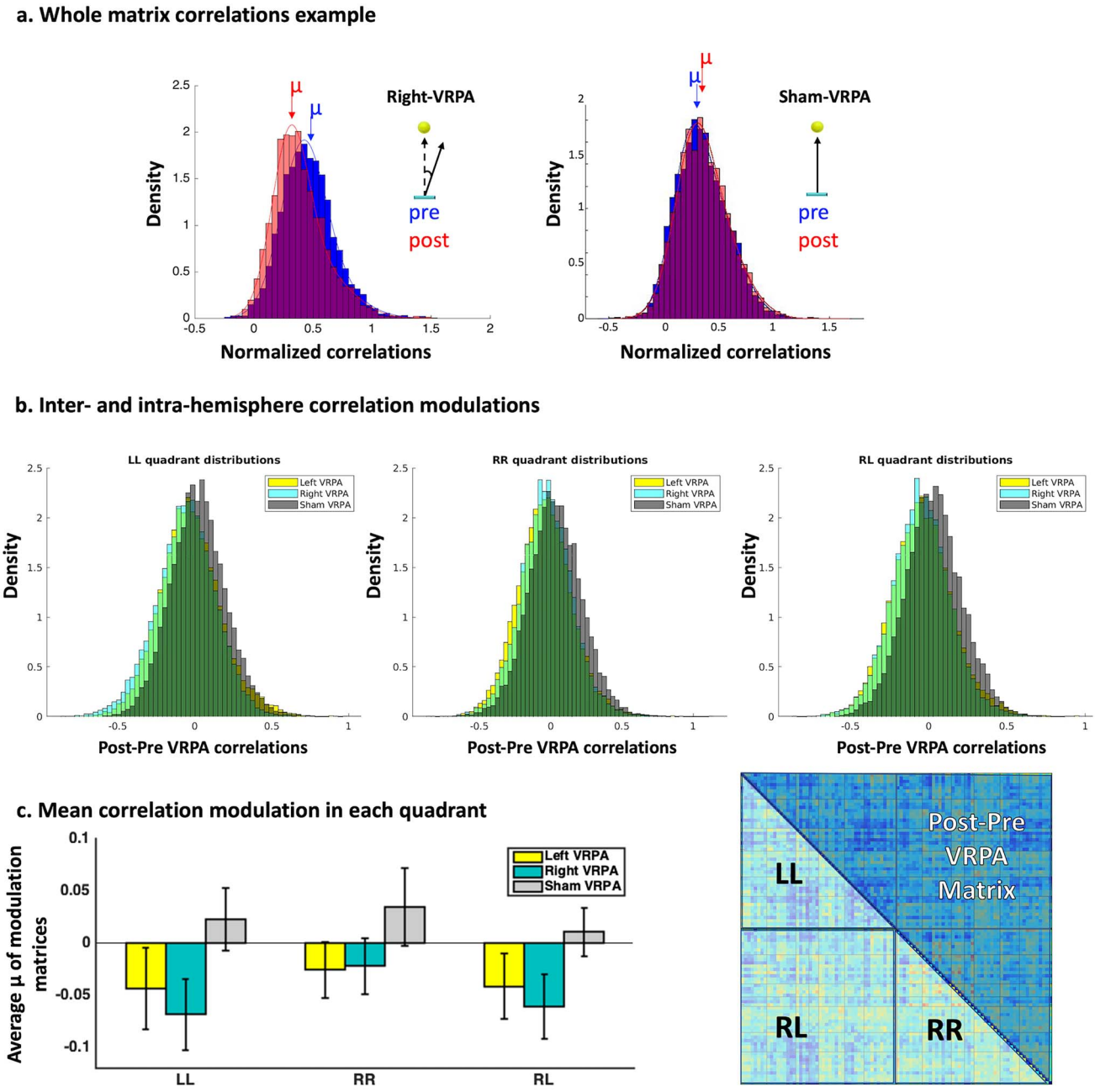

Fig. 4. Gaussian mixture model results for comparing between correlation matrices. a) Single participants example (from the right-VRPA and the sham-VRPA groups), showing the distribution of correlation values in the connectivity matrix (Fisher's Z normalized) pre- and post- VRPA. A mixture of 2 Gaussians was fitted to each distribution, from which a μ value representing the mean was extracted and used for further statistical analysis. b) Connectivity modulations across hemispheres. Distribution of mean modulation matrix values (post–pre VRPA) in the 3 groups in each of the possible connectivity types—within left hemisphere (left; LL), within right hemisphere (middle; RR), and between hemispheres (right; RL). c) left side: average μ value of modulation matrices across participants in each quadrant for each group (errorbars denote standard error of the mean (SEM) across participants). Right: a schematic example of modulation matrix with an annotation of the submatrices representing each quadrant.

quadrants, we then performed a 2-way mixed-effects ANOVA on the individual participant modulation matrices with factors group (left/right/sham VRPA) and quadrant (LL/RR/RL) and found a main effect of quadrant (Fig. 4c; $F(2,80) = 4.6$; $P = 0.013$). In post-hoc tests, we did not find any significant difference between left- and right-VRPA, and the mu modulation values in each quadrant were not significantly different from zero (smallest $P = 0.064$ for right-VRPA LL quadrant). Nevertheless, these results suggest that indeed a slightly (though not significantly) different modulation was induced in each hemisphere and across hemispheres.

Finally, in order to establish a link between the form of VR-mediated sensorimotor adaptation introduced here and the classic PA, we compared resting-state data from the present sample of participants performing VRPA and an independent group of participants exposed to standard PA procedure. To that end, we generated similar connectivity matrices from our previously published data, in which resting state fMRI was collected before and after a brief exposure to rightward-shifting PA goggles (see Wilf et al. 2019; Gudmundsson et al. 2020 for details). We found that resting-state modulations were strikingly similar following either VRPA or

PA (Supplementary Fig. 1a, see online supplementary material for a color version of this figure). Namely, reductions in connectivity between the DMN and the attentional networks including IFG and STS regions. A qualitative visual inspection again suggested more pronounced connectivity decreases within the left hemisphere and between left and right hemispheres, evident following both right-VRPA and right-PA exposure. This finding suggests a lateral bias towards decreases in left hemisphere connectivity, similarly to the modulation we found following right VRPA. Repeating the gaussian mixture model separate quadrants analysis while including the group who trained with standard rightward PA yielded comparable results, with right PA group showing high similarity to the right and left VRPA groups (Supplementary Fig. 1b, see online supplementary material for a color version of this figure; main effect of quadrant: $F(2,106) = 5.34$, $P = 0.006$). A 2-way ANOVA comparing only right-PA to right-VRPA showed no difference between the groups ($F(1,26) = 0{,}153$; $P = 0.669$).

Taken together, the pattern of VRPA-induced modulations suggests an overall decrease in spontaneous resting-state connectivity, with more pronounced reductions in the hemisphere opposite to that of the shift induced by the sensorimotor training, mainly between DMN and attentional regions.

VRPA effects on brain activity while processing naturalistic visual stimuli

After establishing VRPA effects on spontaneous activity, we tested whether the training-induced modulation of brain activity would also affect stimulus-induced responses naturalistic stimuli, namely movie scenes. To that end, we compared the cortical responses with free-viewing of an identical series of short videos before and after VRPA training (see Fig. 1c). The videos contained salient moving objects either on the left side, right side, or both sides of the screen. This task was performed only for the right-VRPA group and the sham-VRPA group (see Task 2 in the Methods). Supplementary Fig. 2 shows the pattern of activation in the right-VRPA group in response to the entire set of videos, separately for pre and post VRPA phases. As expected from naturalistic stimulation, in both pre and post phases, the activation spanned the entire hierarchy of visual processing, including parietal and frontal attentional regions (Supplementary Fig. 2, see online supplementary material for a color version of this figure; consistent with Nardo et al. 2016). Crucially, an enhancement of activity emerged after the right VRPA training, specifically in the right visual cortex (Supplementary Fig. 2, see online supplementary material for a color version of this figure; green-black arrow).

Indeed, a direct contrast between pre- and post-VRPA activation maps revealed a significant increase of response to naturalistic videos in an area within the parieto-occipital sulcus (POS; Fig. 5a; MNI coordinates [20, −65, 24]). This enhancement was confined to the right hemisphere, whereas left hemisphere activation pattern remained similar to the pattern found prior to adaptation. Thus, visual activation following right-VRPA was biased in favor of the right hemisphere, suggesting enhanced representation of the left portion of space. We further investigated whether this modulation depended on the spatial distribution of salient stimuli in the movies (i.e. left-lateralized/right-lateralized/bilateral), or it was generalized across all video categories. When examining the different video categories separately, we found a strikingly robust effect across the video categories, with the same POS region showing enhanced activation in right-lateralized, left-lateralized, and both types of bilateral videos (Fig. 5b). An ROI analysis comparing between the pre- and post-beta values in right POS across the different conditions confirmed this observation: A 2-way repeated-measures ANOVA with factors phase (pre/post) and condition (leftLat/rightLat/leftBil/rightBil) showed a significant main effect of phase ($F(1,14) = 64.31$; $P < 0.001$), no main effect of condition ($F(3,42) = 0.113$; $P = 0.95$), and no interaction (Fig. 5c). Thus, the right hemisphere visual area responded more to naturalistic stimuli following right-VRPA, regardless of whether the salient object appeared on the left or right side of the screen.

Next, to probe for a link between neural and behavioral aftereffects, we compared the change in right POS activity during movie presentation ("all videos" condition) to the change in the pointing straight-ahead accuracy (assessing subjective body midline) between pre- and post- right-VRPA. We found a striking correlation between the extent of leftward deviation in subjective body midline induced by VRPA and the size of modulation of right POS activity while processing naturalistic visual stimuli ($r = 0.68$; $P = 0.005$; Fig. 5d). This result provides a strong link between the effect of VRPA on sensorimotor realignment and its effect on naturalistic visual processing.

A similar analysis was applied for the sham group to control for test–retest effects. The comparison of movie-evoked brain activity between pre- and post-sham-VRPA showed only an inconsistent enhancement in bilateral intraparietal sulcus (IPS) regions. This effect was not consistent across movie categories, i.e. it was present only for right-salient bilateral videos, and was not correlated to behavioral results (Supplementary Fig. 3a and b, see online supplementary material for a color version of this figure). To verify the specificity of right POS modulation to real VRPA training, we tested whether activity in right POS ROI was also modulated by sham-VRPA, and found no modulation ($P = 0.48$; paired t-test between pre and post). Correspondingly, no correlation was found between changes in pointing bias and changes in beta values pre and post sham-VRPA, neither for IPS nor for right POS betas (Supplementary Fig. 3c, see online supplementary material for a color version of this figure).

Finally, we further investigated how the changes in evoked activity induced by right-VRPA in the right POS during videos presentation were related to changes in its connectivity with other brain regions, using a PPI analysis. We found that at the "pre" session (before right VRPA training), the right POS area showed no significant interactions with other areas. However, following right-VRPA, the right POS showed significant interactions with left IPL region and bilateral STS regions (Fig. 6). These areas are part of the DMN network (Fig. 6; green shades), which also demonstrated changes in connectivity following VRPA in the resting state connectivity analyses described above (see Fig. 3c and Section "Resting state connectivity"). This suggests that the enhancement of POS activation in the right-VRPA group was modulated by interactions with DMN regions in the left IPL and bilateral STS. PPI analysis yielded no significant interactions in either the "pre" or "post" sessions in the sham-VRPA group (taking as seed region the IPS; see Section "Methods").

Discussion

VRPA successfully induced sensorimotor adaptation in healthy participants, as demonstrated by long lasting proprioceptive-motor aftereffects. These behavioral effects were associated with modulations in resting-state connectivity patterns, namely reduced connectivity between DMN/FPN and attentional networks, more pronouncedly in the hemisphere contralateral to the VRPA deviation. The training-induced modulations were

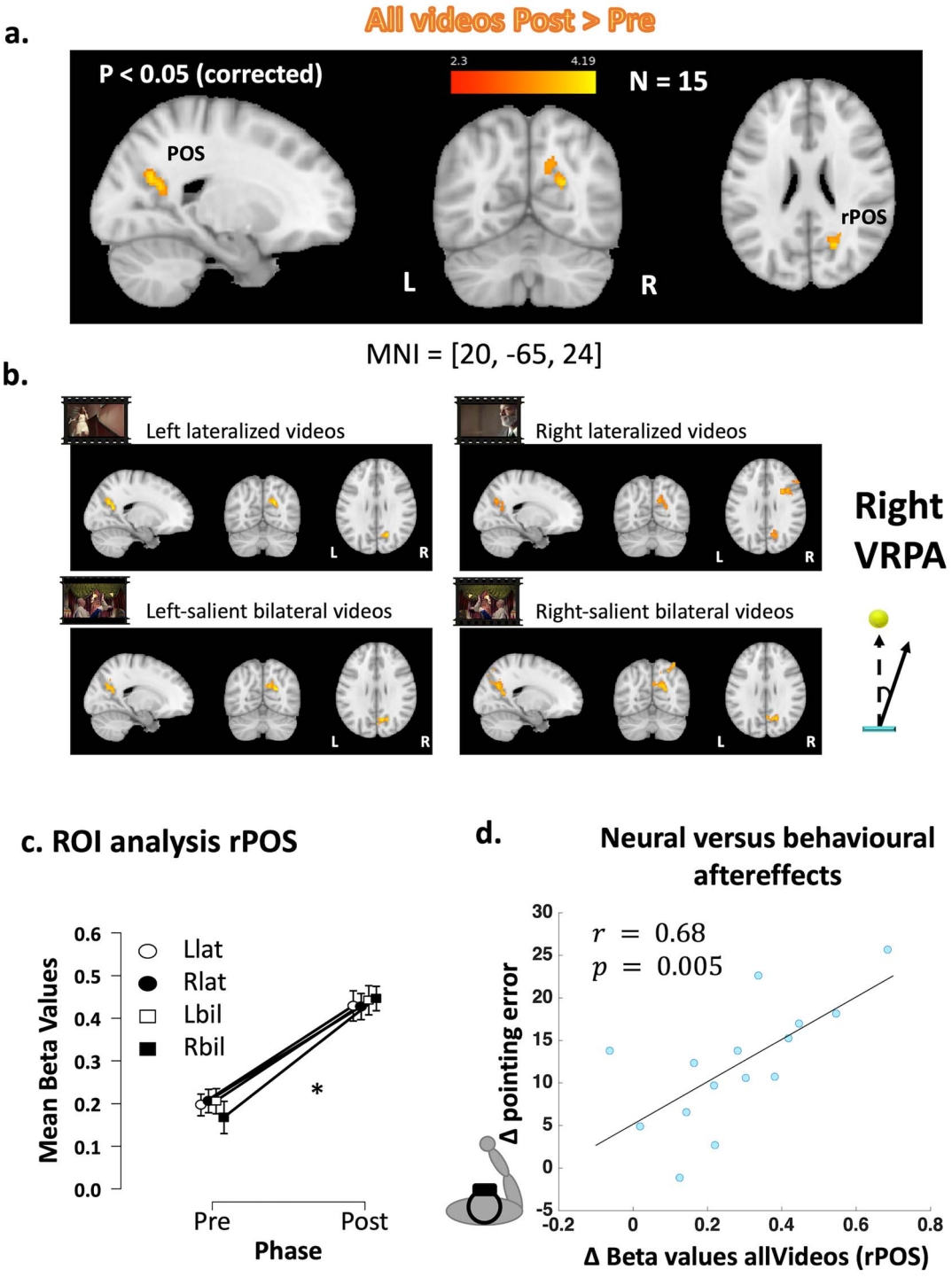

Fig. 5. Right VRPA upregulates responses to naturalistic videos in the right POS. a) Direct contrast between post–pre activation maps in response to all types of videos revealed enhanced activation in the right POS following right VRPA. Colorbar applies to all maps b) Contrast between post–pre activation maps in response to each video type. Right POS is consistently modulated. c) Mean beta values of rPOS pre- and post- right-VRPA across video conditions. Errorbars denote SEMs. Llat = left lateralized; Rlat = right lateralized; Lbil = left bilateral; Rbil = right biletaral d) Correlation between Neural and behavioral aftereffects of right-VRPA. The scatter plot demonstrates the relation between (x-axis) the change in rPOS activity in response to all video types in each participant (N = 15), versus (y-axis) the change in pointing error in the manual straight ahead task between pre- and post- right-VRPA (positive values here denote a more extensive leftward deviation in pointing movements in the post- session). rPOS = right Parieto-Occipital Sulcus.

not confined to spontaneous activity, but affected also cortical responses to free viewing of naturalistic videos. Rightward-VRPA training enhanced visual responses in a retinotopic area within the right POS, presumably reflecting enhanced visual responses to the left portion of space. Moreover, this hemispheric bias in visual responses was directly linked to the behavioral aftereffect, as the extent of upregulation of right POS activity during naturalistic viewing was highly correlated with the extent of leftward proprioceptive-motor biases induced by VRPA. Finally, PPI analyses showed that the right POS region interacted with DMN

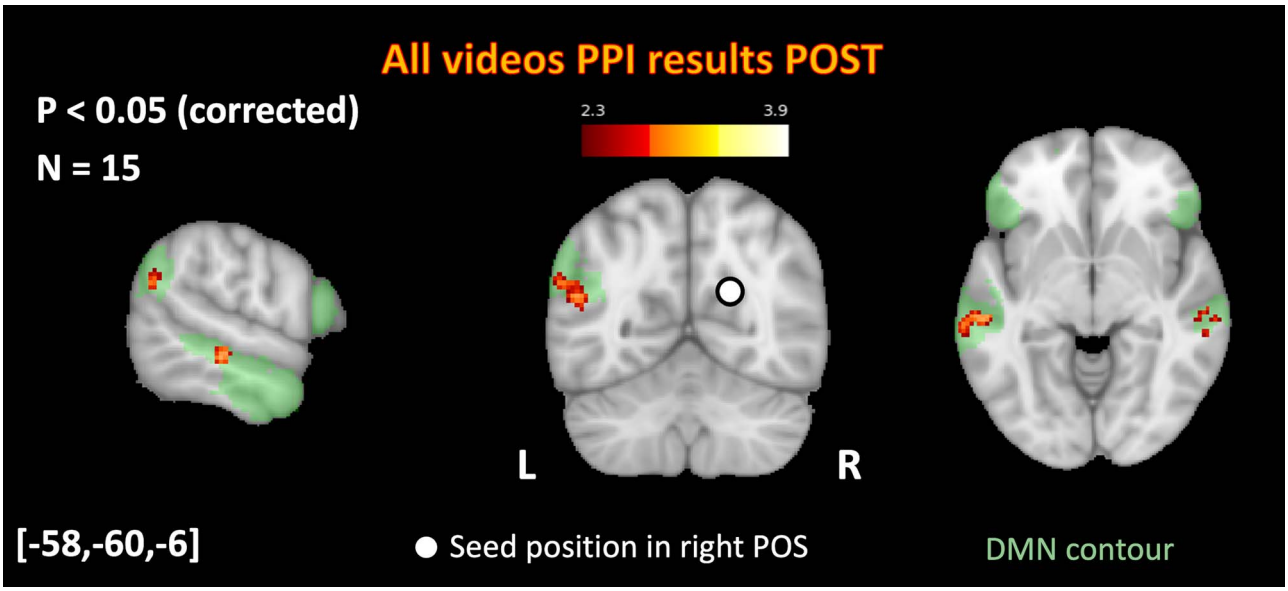

Fig. 6. PPI analysis with right POS after right-VRPA. Clusters in orange show areas that significantly interact with right POS seed (same region as in Fig. 5) during video presentation following right-VRPA. Areas include bilateral STS and left IPL. Light green contour shows DMN-b subnetwork as depicted in Yeo et al. (2011) 17-network parcellation (network #17). Numbers in brackets represent MNI slices coordinates.

areas in the IPL and STS during naturalistic viewing only following right-VRPA, suggesting that changes in visual areas processing naturalistic stimuli following VRPA were mediated by these high-level, heteromodal regions. We will discuss possible interpretation and limitations of each of these results separately, and eventually suggest a model for VRPA-induced brain modulations, with potential implications for neglect rehabilitation.

Unbalancing resting state connectivity between DMN and attentional areas

Our finding of an enhanced decoupling between DMN/FPN regions and dorsal and ventral attentional networks after VRPA (see Fig. 3c), more pronounced in the hemisphere contralateral to the shift, is consistent with recent studies that measured standard PA aftereffects in resting state connectivity (Schintu et al. 2019; Tsujimoto et al. 2019; Wilf et al. 2019; Gudmundsson et al. 2020). Nevertheless, we acknowledge that the network labeling of the atlas ROIs used in the current study might be crude since some ROIs (especially those of larger size) might have subclusters in more than one network (e.g. different IPL subregions are part of DMN, DAN, and VAN). However, for the sake of simplicity we chose to use this approximation and label each ROI according to the network most overlapping with it. Nevertheless, the resemblance between VRPA and PA connectivity modulations (see also Supplementary Fig. 1, online supplementary material for a color version of this figure) highlights the mechanism by which visuomotor adaptation shapes brain connectivity, in both VR and non-VR settings. We suggest that the bottom-up learning process during adaptation eventually propagates forward in the processing pathway to affect high-level, heteromodal, cortical networks. In terms of functionality, the decoupling between DMN and attention networks is crucial for execution of goal directed behavior (Dixon et al. 2017; for more elaborated discussion see Wilf et al. 2019), and the extent of DMN deactivation was previously found to be correlated with learning parameters in a visuomotor adaptation task (Cassady et al. 2018). In addition, STS (Luauté et al. 2009) and IFG (Baldauf and Desimone 2014) regions were found to be consistently related to spatial adaptation paradigms.

Furthermore, the pattern of the hemispheric laterality visible from the connectivity modulation matrices (also that of the standard PA) suggests a VRPA-induced spatial realignment and a shift in reference frame, reflecting at the brain level the mechanisms underlying PA at the behavioral level (see Redding and Wallace 1996; Prablanc et al. 2020). This is corroborated by the fact that connectivity changes were found in networks responsible for spatial allocation of attention, such as the ventral and dorsal attentional networks (Corbetta and Shulman 2002). The visuo-spatial attention system shows lateralization that manifests both in fMRI connectivity (Smith et al. 2009) and behaviorally in inherent lateral spatial biases in healthy individuals ("pseudoneglect"; Bowers and Heilman 1980). Correspondingly, we found slightly stronger behavioral aftereffects following left- as compared with right-VRPA, similarly to previous findings with standard PA (Michel et al. 2008). This dependency on the direction of the adaptation shift is largely in line with recent findings on rightward and leftward standard PA (Schintu et al. 2019; Tsujimoto et al. 2019), who found connectivity modulations in parieto-frontal attentional regions as a function of the shift direction. Findings from standard PA paradigms show also hemispheric laterality in task-induced aftereffects. For instance, Crottaz-Herbette et al., showed that right and left PA produced hemisphere-specific activation modulation in IPL region during a visual attention task (Crottaz-Herbette et al. 2014, 2017b). Nevertheless, we acknowledge that in the current study, the differences in modulations between quadrants did not reach statistical significance, possibly because of insufficient statistical power. Therefore, this specific effect will require further replications in the future with larger sample sizes.

In the sham group, only slight increases in connectivity between visuomotor areas were found following training. These results are in line with the notion that sham-VRPA, without a visuomotor discrepancy, actually corresponds to an intensive multisensory-motor training in VR. Thus, the resting state patterns seem to resonate the co-activation between visual and

motor areas that occur during the training (cf. Albert et al. 2009; Guerra-Carrillo et al. 2014).

In summary, exposure to VRPA modulated resting-state connectivity in high-level, heteromodal, cortical networks, in a way that reflects the spatial shift in reference frame induced by the training. In the next sections, we will propose a mechanism by which these connectivity modulations might affect processing of external sensory stimuli.

Upregulation of right POS activation during naturalistic viewing

Previous studies assessed brain activity following PA during visual attention, auditory detection, and working memory tasks (Crottaz-Herbette et al. 2014; Tissieres et al. 2018). For example, Martín-Arévalo et al. (2016) used a Posner task and event-related potentials to track fine modulation of brain activation and reaction times after PA. Specifically after left PA, they reported larger decrease of event-related potentials in response to left, compared with right, cues. Given that the origin of this event-related potential is linked to the intraparietal sulcus and to the process of attentional orienting, this finding was interpreted as reflecting an orienting bias towards rightward cues following left PA. However, lab-designed task-induced activity does not correspond to the complexity of signals emerging in real life conditions (Nastase et al. 2020). For this reason, in the current study, we recorded brain activity that was not confounded by a goal-directed task, but rather entailed implicit processing related to everyday life stimuli, as portrayed by the naturalistic videos. This approach allowed us to bridge the gap between previous results produced in highly controlled, but artificial laboratory conditions, and adaptation aftereffects in real-life-like perception, that are difficult to measure. Despite the free-flowing nature of the experience, natural viewing reliably represents sensory perception, since movie-induced brain activity is largely consistent between individuals and between movie repetitions within the same individual (Hasson et al. 2004, 2010; Wilf et al. 2017; Strappini et al. 2019).

Our results highlighted the POS area as a target of VRPA-induced, but not sham-VRPA-induced, modulations during processing of naturalistic stimuli. This retinotopic area has a role in peripheral peripersonal space representation (Galletti et al. 1999), in particular during reaching or visuomotor tracking of target errors (Diedrichsen et al. 2005). Of particular interest is the finding that POS is a key player in PA process; according to a study by Luauté et al. (2009), POS activation is responsible for successful error correction during PA exposure, suggesting that it contributes to the strategic component of adaptation. Furthermore, the fact that in our study POS area was activated especially in the right hemisphere could be interpreted as an enhanced representation of the left portion of space following rightward adaptation. Though in the present study, the analyses of naturalistic stimuli processing were limited to the rightward-VRPA group, future studies examining the effect of leftward-VRPA will determine whether the laterality of the neural aftereffects is dependent upon the directionality of the reference frame shift (i.e. by demonstrating symmetrical neural aftereffects), or it is generally lateralized to the right hemisphere.

A possible confounding factor that could influence our results is the fact that participants viewed the same exact set of videos twice, namely that there was a test–retest effect. However, data from the sham-VRPA group, who underwent exactly the same experimental paradigm, but without any adaptation shift, showed only highly inconsistent bilateral activity increases in the IPS area, and no effect on rPOS. Since the IPS area is highly activated both during reaching movements and during movie viewing (Culham et al. 2003; Goldberg et al. 2014; Nardo et al. 2016), one option is that this effect resonates activations of visuomotor practice during the sham training, as reflected also in a slight increase in visuomotor resting state connectivity (Fig. 3c; right).

Since participants were free to move their eyes during video presentation, another potential interpretation of our results is that the right POS enhancement after VRPA was due to differences in eye movement scanning patterns between pre- and post- VRPA training sessions (e.g. tendency to saccade more to the left after adaptation; as demonstrated for neglect patients in Serino et al. 2006). Unfortunately, we could not monitor eye movements in the scanner, so we cannot directly confirm, nor exclude this hypothesis. Relatedly, a recent study by Gilligan et al. (2019) found that PA had no effect on subsequent gaze directions in healthy individuals during passive gazing, but only when gazing involved active arm movements. However, the simplicity of the display presented in Gilligan et al., and the presence of a task at hand might have covered such an effect, which may manifest in more naturalistic and dynamical environments such as those used in the current study. Moreover, theoretically, only videos that presented bilateral salient objects actually lead to a competition between execution of left or right saccades (Nardo et al. 2016), whereas unilateral videos naturally drew gaze to the only salient moving stimulus on the screen. Therefore, the fact that the right hemisphere POS enhancement was evident for both left and right unilateral videos suggests that the neural aftereffects did not rely solely on differences in saccade directions. Instead, we suggest that the right POS upregulation might have stemmed from top-down influences from areas related to reference frame transformation and attention allocation, leading to an enhancement of left hemispace visual processing (Cohen and Andersen 2002; Kim and Kastner 2019).

Link between neural and behavioral aftereffects

A first indirect support for this hypothesis comes from the correlation between the behavioral aftereffects measured in the straight-ahead pointing task and the upregulation of the right POS during naturalistic stimuli processing. Pointing straight ahead task is a common tool for assessing egocentric lateral spatial biases in both healthy individuals and neglect patients, representing proprioceptive-only effects (Bultitude et al. 2021), independent of any visual context (Karnath 1994; Fleury et al. 2019). On the other hand, the movie viewing task was purely perceptual, and did not involve any manual or proprioceptive components. Thus, the fact that the magnitude of proprioceptive bias was proportional to the magnitude of right POS visual activations upregulation, suggests a common VRPA-induced bias in spatial representation, manifested in both visual perception and proprioception. It is well accepted that PA induces a contralateral shift in reference frame (Redding and Wallace 1996), which generalizes across different tasks (Michel 2015). Thus, we propose that the same effect induced by VRPA manifests both for encoding of incoming stimuli and for movement execution. Similarly, future studies testing purely visual aftereffects tasks, such as the visual straight ahead task, will potentially quantify behaviorally the VRPA-induced visual aftereffect. This change in reference frame might be mediated by top-down influences from higher order heteromodal regions (Cohen and Andersen 2002), as tested via PPI analysis.

Naturalistic stimulus responses relate to connectivity modulation through DMN areas

PPI analysis demonstrated that following rightward VRPA, significant interactions emerged between right POS and areas in the DMN network during movies presentation, in areas that also showed VRPA-related changes in resting state connectivity. More specifically, right POS was found to interact with left IPL and bilateral STS regions (see Fig. 6). Previous studies on PA-related brain activity found that activity in left IPL during visual attention task is modulated by PA in both healthy individuals and neglect patients (Crottaz-Herbette et al. 2014, 2017a). In addition, both IPL and STS change their resting-state connectivity following PA (Wilf et al. 2019). These areas have an important role in the representation of space: STS region is active during the last stages of PA (Luauté et al. 2009), and has been suggested to be the area integrating egocentric and object-centered reference frames (Karnath et al. 2001), while IPL is a key area for reference frames transformation (Cohen and Andersen 2002). IPL lesion results in severe spatial deficits in brain damaged patients (Corbetta et al. 2005), whereas its suppression via TMS results in a lack of PA after-effects in pointing straight ahead (Terruzzi et al. 2021). Recently, a line of transcranial direct current stimulation studies highlighted a cerebello-parietal network that is involved in the recalibration and realignment processes taking place during PA, with posterior parietal cortex (PPC) and cerebellum activation determining the rate of adaptation (Panico et al. 2018, 2022). Using TMS in healthy participants, Schintu et al. (2021) highlighted the role of the posterior parietal cortex in line bisection judgment and visuospatial bias. Theta burst TMS temporarily disrupting the function of the right posterior parietal cortex led to a rightward shift in line bisection judgment, and increased resting state functional connectivity between the right posterior parietal cortex and the left superior temporal gyrus. Based on a correlation with fractional anisotropy within the posterior callosal pathway, the authors highlighted the role of structural interhemispheric connections in their effects. Thus, these high-level IPL and STS regions are likely involved in mediating the shift in reference frames induced by sensorimotor adaption, which manifests multimodally in any spatial task, such as processing of naturalistic movies or pointing straight ahead. These internal biases are evident also in the spontaneous connectivity modulations, in the decoupling of DMN and attentional networks.

Specifically, our results imply that the connectivity changes might bias hemispheric laterality depending on the direction of the adaptation. Therefore, a decrease in connectivity within the left hemisphere following rightward-VRPA might bias DMN connectivity in favor of the right hemisphere. This, in turn, can mediate enhanced activity in the right hemisphere in response to an incoming stimulus (Fig. 7). This view is in line with a recent account of DMN function, namely its role in the integration of past information with current stimulus processing during naturalistic stimulation (Yeshurun et al. 2021). This function is supposed to be mediated by topographic connectivity between DMN and primary visual areas (Knapen 2021), structuring the communication between distant brain regions. Our findings are in accordance with this model, with the addition of demonstrating that this long-range DMN-visual cortex connections adapt in cases of altered spatial representations, such as after VRPA.

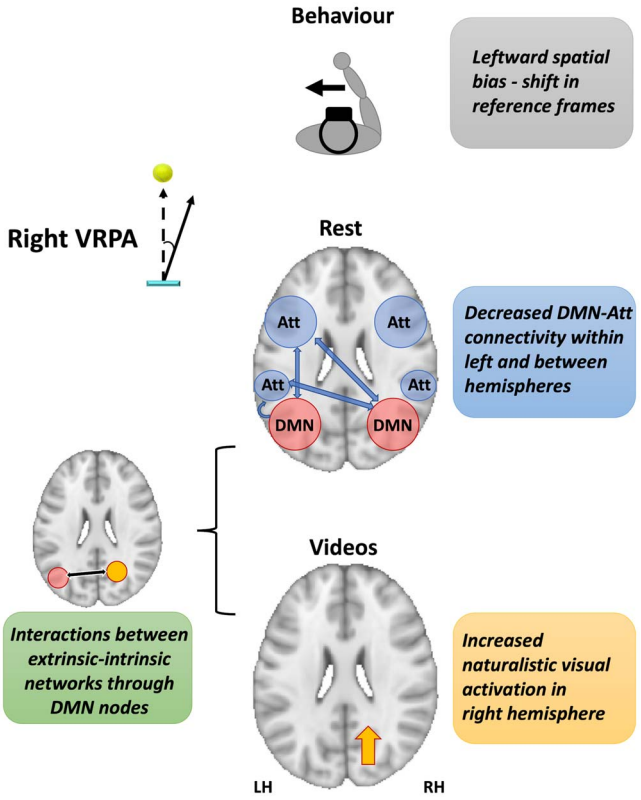

Fig. 7. Schematic model for right-VRPA induced modulations. Bottom-up inputs during right VRPA training realign spatial reference frames to the left side, and propagate to high level regions in the DMN and attentional networks ("Att"). This, in turn, manifests in biases in resting state connectivity between DMN and Att, which then mediates right hemisphere activity increase during naturalistic videos processing.

Potential implications for neglect rehabilitation

Long-range connectivity, mainly between regions of the DMN and the dorsal attentional system, is structurally altered in neglect syndrome, usually following a lesion in right fronto-parietal regions, such as temporo-parietal junction (TPJ; Corbetta et al. 2005; Corbetta and Shulman 2011; Baldassarre et al. 2014). Correspondingly, studies examining the impact of lesion location on the efficacy of PA showed that responders to PA have preserved posterior callosal pathway and preserved right superior parietal lobule SPL (Chen et al. 2014; Tissieres et al. 2017; Goedert et al. 2018; Saj et al. 2019; Gutierrez-Herrera et al. 2020). These unilateral lesions result in a general imbalance of functional connectivity between hemispheres (Lunven and Bartolomeo 2017), which is proportional to the level of spatial impairment (Ptak et al. 2020). Accordingly, neglect recovery is associated to the re-emergence of decoupling between DMN and attentional networks within and across hemispheres (Ramsey et al. 2016). We propose that PA, and its current extension in VRPA, can modulate exactly these large-scale networks in favor of recreating connectivity changes similar to those evident during spontaneous recovery (see also Wilf et al. 2019). Importantly, the hemispheric laterality found in the connectivity modulations implies that this tool can be used, at least partially, to re-balance aberrant connectivity in neglect patients via compensatory mechanisms in the left DMN-attentional networks connectivity and the right visual cortex (Crottaz-Herbette et al. 2017a; Robineau et al. 2019). Furthermore, VRPA might offer a more accessible and easily-controlled manner to study the neural basis of adaptation in MRI settings, in both neglect patients and healthy participants (see Bultitude et al. 2017). In the past few years VRPA protocols have been tested in healthy and brain damaged populations in an effort to assess their validity, sometimes with inconsistent effects:

Cho et al. (2020, 2022) used a depth-sensing camera to track hand movements, while recreating classic PA settings in VR. Bourgeois et al. (2021) used a static array of targets in VR, while applying visuomotor rotation on the position of a rod representing the hand to simulate PA, and found, in neglect patients, subsequent spatial biases in motor bisection tasks, but not in purely perceptual tasks (see also Gammeri et al. 2018 for similar results in healthy individuals). We have previously developed a robot-based VRPA paradigm, which implements visuomotor rotation while actively or passively performing reaching movements to static targets in a naturalistic VR environment (Wilf et al. 2021). In the present study, our novel VRPA setup was designed to reproduce naturalistic ecological conditions with HMD settings maintaining portability and ease of use—with the participant's hand being embodied as a virtual hand, and 3-dimensional hand and target movements promoting natural behavior (e.g. Carter et al. 2016). Hence, the present VR setup has enabled us to tap into sensorimotor mechanisms that are more ecological than during standard PA and other previous digitalization of PA (e.g. by reaching to dynamic naturalistic objects), thus potentially resulting in better transfer to real-life behavior (Fortis et al. 2010; Champod et al. 2018). Though the adaptation shift was implemented using visuomotor rotation (cf. Krakauer 2009; Gammeri et al. 2018), the fact that the feedback from the hand position was limited only to the last part of the movement (where the lateral shift was already close to its maximum size) promotes explicit adaptation mechanisms (Taylor et al. 2014), resembling that of the classic PA (Wilf et al. 2021). Ramos et al. (2019) addressed this issue directly by comparing between adaptation induced by horizontal displacement and visuomotor rotation manipulations, and found comparable adaptation aftereffects, that were both larger than those induced by PA goggles.

In terms of visual processing, although the visual cortex is usually spared in patients with neglect without hemianopia, interferences in primary visual cortex activity were still found in certain cases (Vuilleumier et al. 2008). The right hemisphere enhancement we found following adaptation suggests that VRPA could potentially boost the damaged right visual cortex activation in neglect patients, through top-down modulations by fronto-parietal regions (Corbetta and Shulman 2011). Naturalistic movies are a powerful tool to uncover pathologies in perception and biases in spatial orientation in the absence of an explicit task (cf. Machner et al. 2012; Nardo et al. 2019). Therefore, naturalistic stimuli can serve as a probe for daily-life perception and potential biases in spatial representations in neglect patients, and consequently track the potential re-balancing effect of VRPA rehabilitation training in these patients.

Conclusions

We demonstrated a rapid realignment of cortical activity and connectivity following virtual reality-based prism-like sensorimotor adaptation (VRPA), correlated to reference frame shift as captured by behavioral spatial biases measurements. We suggest that VRPA training induces decoupling between large-scale brain networks (the DMN and attentional networks), with hemispheric laterality depending on the direction of the adaptation shift. This connectivity modulation then mediates a low-level bias in responses to incoming naturalistic visual inputs as shown by increased response of the ipsilateral visual cortex, in proportion to the measured behavioral spatial biases. Our results show bottom-up propagation of sensorimotor training affecting high-level functional networks, which in turn induce top-down modulations on sensory processing. These findings might have meaningful implications for understanding the mechanisms underlying sensorimotor plasticity in healthy individuals, and for applying VR adaptation training for rehabilitating brain-damaged patients suffering from deficits in spatial representation.

Acknowledgments

The authors thank Samantha Bechet for helpful assistance with data analysis. The authors wish to thank all the participants who took part in the study. The authors thank Antoine Lutti, Giulia Di Domenicantonio, Christine Kieffer, Petr Grivaz, and Giulio Mastria for their help in data acquisition, and Dimitri Van de Ville for helpful comments and feedback on data analysis.

Supplementary Material

Supplementary material is available at *Cerebral Cortex* online.

Funding

This work was supported by the European Union's Horizon 2020 research and innovation programme under the Marie Sklodowska-Curie grant agreement no. 789548 and the Swiss government excellence scholarship to M.W., and the Swiss National Science Foundation grant (grant PP00P3_163951/1) to A.S.

Conflict of interest statement: Celine Dupuis, Sonia Crottaz-Herbette and Andrea Serino have a role in the neuroscience team of Mind-Maze SA.

References

Albert NB, Robertson EM, Miall RC. The resting human brain and motor learning. *Curr Biol*. 2009:19:1023–1027.

Baldassarre A, Ramsey L, Hacker CL, Callejas A, Astafiev SV, Metcalf NV, Zinn K, Rengachary J, Snyder AZ, Carter AR. Large-scale changes in network interactions as a physiological signature of spatial neglect. *Brain*. 2014:137:3267–3283.

Baldauf D, Desimone R. Neural mechanisms of object-based attention. *Science*. 2014:344:424–427.

Berlot E, Popp NJ, Diedrichsen J. A critical re-evaluation of fMRI signatures of motor sequence learning. *Elife*. 2020:9:e55241.

Bourgeois A, Turri F, Schnider A, Ptak R. Virtual prism adaptation for spatial neglect: a double-blind study. *Neuropsychol Rehabil*. 2021: 1–15.

Bowers D, Heilman KM. Pseudoneglect: effects of hemispace on a tactile line bisection task. *Neuropsychologia*. 1980: 18:491–498.

Bultitude JH, Farnè A, Salemme R, Ibarrola D, Urquizar C, O'Shea J, Luauté J. Studying the neural bases of prism adaptation using fMRI: a technical and design challenge. *Behav Res Methods*. 2017:49:2031–2043.

Bultitude JH, Hollifield M, Rafal RD. Patients with lesions to the intraparietal cortex show greater proprioceptive realignment after prism adaptation: evidence from open-loop pointing and manual straight ahead. *Neuropsychologia*. 2021:158:107913.

Carter A, Foreman M, Martin C, Fitterer S, Pioppo A, Connor L, Engsberg J. Inducing visuomotor adaptation using virtual reality gaming with a virtual shift as a treatment for unilateral spatial neglect. *J Intellect Disabil-Diagn Treat*. 2016:4: 170–184.

Cassady K, Ruitenberg M, Koppelmans V, Reuter-Lorenz P, De Dios Y, Gadd N, Wood S, Riascos Castenada R, Kofman I, Bloomberg J. Neural predictors of sensorimotor adaptation rate and savings. *Hum Brain Mapp*. 2018:39:1516–1531.

Champod AS, Frank RC, Taylor K, Eskes GA. The effects of prism adaptation on daily life activities in patients with visuospatial neglect: a systematic review. *Neuropsychol Rehabil*. 2018:28: 491–514.

Chen P, Goedert KM, Shah P, Foundas AL, Barrett A. Integrity of medial temporal structures may predict better improvement of spatial neglect with prism adaptation treatment. *Brain Imaging Behav*. 2014:8:346–358.

Cho S, Kim W-S, Park SH, Park J, Paik N-J. Virtual prism adaptation therapy: protocol for validation in healthy adults. *JoVE (J Visual Exp)*. 2020:156:e60639.

Cho S, Chang WK, Park J, Lee SH, Lee J, Han CE, Paik N-J, Kim W-S. Feasibility study of immersive virtual prism adaptation therapy with depth-sensing camera using functional near-infrared spectroscopy in healthy adults. *Sci Rep*. 2022:12:1–12.

Choi U-S, Kawaguchi H, Matsuoka Y, Kober T, Kida I. Brain tissue segmentation based on MP2RAGE multi-contrast images in 7 T MRI. *PLoS One*. 2019:14:e0210803.

Cohen YE, Andersen RA. A common reference frame for movement plans in the posterior parietal cortex. *Nat Rev Neurosci*. 2002:3: 553–562.

Corbetta M, Shulman GL. Control of goal-directed and stimulus-driven attention in the brain. *Nat Rev Neurosci*. 2002:3:201.

Corbetta M, Shulman GL. Spatial neglect and attention networks. *Annu Rev Neurosci*. 2011:34:569–599.

Corbetta M, Kincade MJ, Lewis C, Snyder AZ, Sapir A. Neural basis and recovery of spatial attention deficits in spatial neglect. *Nat Neurosci*. 2005:8:1603–1610.

Crottaz-Herbette S, Fornari E, Clarke S. Prismatic adaptation changes visuospatial representation in the inferior parietal lobule. *J Neurosci*. 2014:34:11803–11811.

Crottaz-Herbette S, Fornari E, Notter MP, Bindschaedler C, Manzoni L, Clarke S. Reshaping the brain after stroke: the effect of prismatic adaptation in patients with right brain damage. *Neuropsychologia*. 2017a:104:54–63.

Crottaz-Herbette S, Fornari E, Tissieres I, Clarke S. A brief exposure to leftward prismatic adaptation enhances the representation of the ipsilateral, right visual field in the right inferior parietal lobule. *Eneuro*. 2017b:4.5

Culham JC, Danckert SL, De Souza JF, Gati JS, Menon RS, Goodale MA. Visually guided grasping produces fMRI activation in dorsal but not ventral stream brain areas. *Exp Brain Res*. 2003:153:180–189.

Dale A, Greve D, Burock M. Optimal stimulus sequences for event-related fMRI. *NeuroImage*. 1999:9:S33–S33.

Desikan RS, Ségonne F, Fischl B, Quinn BT, Dickerson BC, Blacker D, Buckner RL, Dale AM, Maguire RP, Hyman BT. An automated labeling system for subdividing the human cerebral cortex on MRI scans into gyral based regions of interest. *NeuroImage*. 2006:31:968–980.

Diedrichsen J, Hashambhoy Y, Rane T, Shadmehr R. Neural correlates of reach errors. *J Neurosci*. 2005:25:9919–9931.

Dixon ML, Andrews-Hanna JR, Spreng RN, Irving ZC, Mills C, Girn M, Christoff K. Interactions between the default network and dorsal attention network vary across default subsystems, time, and cognitive states. *NeuroImage*. 2017:147:632–649.

Facchin A, Bultitude JH, Mornati G, Peverelli M, Daini R. A comparison of prism adaptation with terminal versus concurrent exposure on sensorimotor changes and spatial neglect. *Neuropsychol Rehabil*. 2020:30:613–640.

Fleury L, Prablanc C, Priot A-E. Do prism and other adaptation paradigms really measure the same processes? *Cortex*. 2019:119: 480–496.

Fortis P, Maravita A, Gallucci M, Ronchi R, Grassi E, Senna I, Olgiati E, Perucca L, Banco E, Posteraro L. Rehabilitating patients with left spatial neglect by prism exposure during a visuomotor activity. *Neuropsychology*. 2010:24:681.

Fox MD, Zhang D, Snyder AZ, Raichle ME. The global signal and observed anticorrelated resting state brain networks. *J Neurophysiol*. 2009:101:3270–3283.

Galletti C, Fattori P, Gamberini M, Kutz DF. The cortical visual area V6: brain location and visual topography. *Eur J Neurosci*. 1999:11: 3922–3936.

Gammeri R, Turri F, Ricci R, Ptak R. Adaptation to virtual prisms and its relevance for neglect rehabilitation: a single-blind dose-response study with healthy participants. *Neuropsychol Rehabil*. 2018:1–14.

Gauthier B, Bréchet L, Lance F, Mange R, Herbelin B, Faivre N, Bolton TA, Van De Ville D, Blanke O. First-person body view modulates the neural substrates of episodic memory and autonoetic consciousness: a functional connectivity study. *NeuroImage*. 2020:223:117370.

Gilligan TM, Cristino F, Bultitude JH, Rafal RD. The effect of prism adaptation on state estimates of eye position in the orbit. *Cortex*. 2019:115:246–263.

Goedert KM, Chen P, Foundas AL, Barrett A. Frontal lesions predict response to prism adaptation treatment in spatial neglect: a randomised controlled study. *Neuropsychol Rehabil*. 2018.

Goldberg H, Preminger S, Malach R. The emotion–action link? Naturalistic emotional stimuli preferentially activate the human dorsal visual stream. *NeuroImage*. 2014:84:254–264.

Gudmundsson L, Vohryzek J, Fornari E, Clarke S, Hagmann P, Crottaz-Herbette S. A brief exposure to rightward prismatic adaptation changes resting-state network characteristics of the ventral attentional system. *PLoS One*. 2020:15: e0234382.

Guerra-Carrillo B, Mackey AP, Bunge SA. Resting-state fMRI: a window into human brain plasticity. *Neuroscientist*. 2014:20: 522–533.

Gutierrez-Herrera M, Eger S, Keller I, Hermsdörfer J, Saevarsson S. Neuroanatomical and behavioural factors associated with the effectiveness of two weekly sessions of prism adaptation in the treatment of unilateral neglect. *Neuropsychol Rehabil*. 2020:30: 187–206.

Hahamy A, Calhoun V, Pearlson G, Harel M, Stern N, Attar F, Malach R, Salomon R. Save the global: global signal connectivity as a tool for studying clinical populations with functional magnetic resonance imaging. *Brain Connect*. 2014:4:395–403.

Hasson U, Nir Y, Levy I, Fuhrmann G, Malach R. Intersubject synchronization of cortical activity during natural vision. *Science*. 2004:303:1634–1640.

Hasson U, Malach R, Heeger DJ. Reliability of cortical activity during natural stimulation. *Trends Cogn Sci*. 2010:14:40–48.

Jacquin-Courtois S, O'shea J, Luauté J, Pisella L, Revol P, Mizuno K, Rode G, Rossetti Y. Rehabilitation of spatial neglect by prism adaptation: a peculiar expansion of sensorimotor after-effects to spatial cognition. *Neurosci Biobehav Rev*. 2013:37: 594–609.

Jäncke L, Gaab N, Wüstenberg T, Scheich H, Heinze H-J. Short-term functional plasticity in the human auditory cortex: an fMRI study. *Cogn Brain Res*. 2001:12:479–485.

Karnath H-O. Subjective body orientation in neglect and the interactive contribution of neck muscle proprioception and vestibular stimulation. *Brain*. 1994:117:1001–1012.

Karnath H-O, Ferber S, Himmelbach M. Spatial awareness is a function of the temporal not the posterior parietal lobe. *Nature*. 2001:411:950.

Karni A, Meyer G, Jezzard P, Adams MM, Turner R, Ungerleider LG. Functional MRI evidence for adult motor cortex plasticity during motor skill learning. *Nature*. 1995:377:155–158.

Kim NY, Kastner S. A biased competition theory for the developmental cognitive neuroscience of visuo-spatial attention. *Curr Opin Psychol*. 2019:29:219–228.

Knapen T. Topographic connectivity reveals task-dependent retinotopic processing throughout the human brain. *Proc Natl Acad Sci*. 2021:118. e2017032118.

Krakauer JW. Motor learning and consolidation: the case of visuomotor rotation. *Progr Motor Control*. 2009:405–421.

Lewis CM, Baldassarre A, Committeri G, Romani GL, Corbetta M. Learning sculpts the spontaneous activity of the resting human brain. *Proc Natl Acad Sci*. 2009:106:17558–17563.

Luauté J, Schwartz S, Rossetti Y, Spiridon M, Rode G, Boisson D, Vuilleumier P. Dynamic changes in brain activity during prism adaptation. *J Neurosci*. 2009:29:169–178.

Lunven M, Bartolomeo P. Attention and spatial cognition: neural and anatomical substrates of visual neglect. *Ann Phys Rehabil Med*. 2017:60:124–129.

Machner B, Dorr M, Sprenger A, von der Gablentz J, Heide W, Barth E, Helmchen C. Impact of dynamic bottom-up features and top-down control on the visual exploration of moving real-world scenes in hemispatial neglect. *Neuropsychologia*. 2012:50: 2415–2425.

Marques JP, Kober T, Krueger G, van der Zwaag W, Van de Moortele P-F, Gruetter R. MP2RAGE, a self bias-field corrected sequence for improved segmentation and T1-mapping at high field. *NeuroImage*. 2010:49:1271–1281.

Martín-Arévalo E, Schintu S, Farnè A, Pisella L, Reilly KT. Adaptation to leftward shifting prisms alters motor interhemispheric inhibition. *Cereb Cortex*. 2016:28:528–537.

Michel C. Beyond the sensorimotor plasticity: cognitive expansion of prism adaptation in healthy individuals. *Front Psychol*. 2015:6:1979.

Michel C, Vernet P, Courtine G, Ballay Y, Pozzo T. Asymmetrical after-effects of prism adaptation during goal oriented locomotion. *Exp Brain Res*. 2008:185:259–268.

Murphy K, Fox MD. Towards a consensus regarding global signal regression for resting state functional connectivity MRI. *NeuroImage*. 2017:154:169–173.

Nardo D, Console P, Reverberi C, Macaluso E. Competition between visual events modulates the influence of salience during free-viewing of naturalistic videos. *Front Hum Neurosci*. 2016: 10:320.

Nardo D, De Luca M, Rotondaro F, Spanò B, Bozzali M, Doricchi F, Paolucci S, Macaluso E. Left hemispatial neglect and overt orienting in naturalistic conditions: role of high-level and stimulus-driven signals. *Cortex*. 2019:113:329–346.

Nastase SA, Goldstein A, Hasson U. Keep it real: rethinking the primacy of experimental control in cognitive neuroscience. *NeuroImage*. 2020:222:117254.

Panico F, Sagliano L, Grossi D, Trojano L. Bi-cephalic parietal and cerebellar direct current stimulation interferes with early error correction in prism adaptation: toward a complex view of the neural mechanisms underlying visuomotor control. *Cortex*. 2018:109:226–233.

Panico F, Rossetti Y, Trojano L. On the mechanisms underlying Prism Adaptation: a review of neuro-imaging and neuro-stimulation studies. *Cortex*. 2020:123:57–71.

Panico F, Sagliano L, Sorbino G, Trojano L. Engagement of a parieto-cerebellar network in prism adaptation. A double-blind high-definition transcranial direct current stimulation study on healthy individuals. *Cortex*. 2022:146:39–49.

Power JD, Mitra A, Laumann TO, Snyder AZ, Schlaggar BL, Petersen SE. Methods to detect, characterize, and remove motion artifact in resting state fMRI. *NeuroImage*. 2014:84:320–341.

Prablanc C, Panico F, Fleury L, Pisella L, Nijboer T, Kitazawa S, Rossetti Y. Adapting terminology: clarifying prism adaptation vocabulary, concepts, and methods. *Neurosci Res*. 2020:153:8–21.

Ptak R, Bourgeois A, Cavelti S, Doganci N, Schnider A, Iannotti GR. Discrete patterns of cross-hemispheric functional connectivity underlie impairments of spatial cognition after stroke. *J Neurosci*. 2020:40:6638–6648.

Ramos AA, Hørning EC, Wilms IL. Simulated prism exposure in immersed virtual reality produces larger prismatic after-effects than standard prism exposure in healthy subjects. *PLoS One*. 2019:14.5. e0217074.

Ramsey LE, Siegel JS, Baldassarre A, Metcalf NV, Zinn K, Shulman GL, Corbetta M. Normalization of network connectivity in hemispatial neglect recovery. *Ann Neurol*. 2016:80:127–141.

Redding GM, Wallace B. Adaptive spatial alignment and strategic perceptual-motor control. *J Exp Psychol Hum Percept Perform*. 1996:22:379.

Robineau F, Saj A, Neveu R, Van De Ville D, Scharnowski F, Vuilleumier P. Using real-time fMRI neurofeedback to restore right occipital cortex activity in patients with left visuo-spatial neglect: proof-of-principle and preliminary results. *Neuropsychol Rehabil*. 2019:29:339–360.

Saj A, Cojan Y, Assal F, Vuilleumier P. Prism adaptation effect on neural activity and spatial neglect depend on brain lesion site. *Cortex*. 2019:119:301–311.

Schintu S, Pisella L, Jacobs S, Salemme R, Reilly KT, Farnè A. Prism adaptation in the healthy brain: the shift in line bisection judgments is long lasting and fluctuates. *Neuropsychologia*. 2014:53: 165–170.

Schintu S, Freedberg M, Gotts SJ, Cunningham CA, Alam ZM, Shomstein S, Wassermann EM. Prism adaptation modulates connectivity of the intraparietal sulcus with multiple brain networks. *Cerebral Cortex*. 30.9 2020:4747–4758.

Schintu S, Cunningham CA, Freedberg M, Taylor P, Gotts SJ, Shomstein S, Wassermann EM. Callosal anisotropy predicts attentional network changes after parietal inhibitory stimulation. *NeuroImage*. 2021:226:117559.

Serino A, Angeli V, Frassinetti F, Làdavas E. Mechanisms underlying neglect recovery after prism adaptation. *Neuropsychologia*. 2006:44:1068–1078.

Siegel JS, Ramsey LE, Snyder AZ, Metcalf NV, Chacko RV, Weinberger K, Baldassarre A, Hacker CD, Shulman GL, Corbetta M. Disruptions of network connectivity predict impairment in multiple behavioral domains after stroke. *Proc Natl Acad Sci*. 2016:113:E4367–E4376.

Smith SM, Fox PT, Miller KL, Glahn DC, Fox PM, Mackay CE, Filippini N, Watkins KE, Toro R, Laird AR. Correspondence of the brain's functional architecture during activation and rest. *Proc Natl Acad Sci*. 2009:106:13040–13045.

Strappini F, Wilf M, Karp O, Goldberg H, Harel M, Furman-Haran E, Golan T, Malach R. Resting-state activity in high-order visual areas as a window into natural human brain activations. *Cereb Cortex*. 2019:29:3618–3635.

Tambini A, Ketz N, Davachi L. Enhanced brain correlations during rest are related to memory for recent experiences. *Neuron*. 2010:65:280–290.

Taylor JA, Krakauer JW, Ivry RB. Explicit and implicit contributions to learning in a sensorimotor adaptation task. *J Neurosci*. 2014:34: 3023–3032.

Terruzzi S, Crivelli D, Pisoni A, Mattavelli G, Lauro LJR, Bolognini N, Vallar G. The role of the right posterior parietal cortex in prism adaptation and its aftereffects. *Neuropsychologia*. 2021:150: 107672.

Tissieres I, Elamly M, Clarke S, Crottaz-Herbette S. For better or worse: the effect of prismatic adaptation on auditory neglect. *Neural Plast*. 2017.

Tissieres I, Fornari E, Clarke S, Crottaz-Herbette S. Supramodal effect of rightward prismatic adaptation on spatial representations within the ventral attentional system. *Brain Struct Funct*. 2018:223: 1459–1471.

Tootell RB, Reppas JB, Dale AM, Look RB, Sereno MI, Malach R, Brady TJ, Rosen BR. Visual motion aftereffect in human cortical area MT revealed by functional magnetic resonance imaging. *Nature*. 1995:375:139–141.

Tsujimoto K, Mizuno K, Nishida D, Tahara M, Yamada E, Shindo S, Kasuga S, Liu M. Prism adaptation changes resting-state functional connectivity in the dorsal stream of visual attention networks in healthy adults: a fMRI study. *Cortex*. 2019:119: 594–605.

Tyszka JM, Kennedy DP, Paul LK, Adolphs R. Largely typical patterns of resting-state functional connectivity in high-functioning adults with autism. *Cereb Cortex*. 2014:24:1894–1905.

Vuilleumier P, Schwartz S, Verdon V, Maravita A, Hutton C, Husain M, Driver J. Abnormal attentional modulation of retinotopic cortex in parietal patients with spatial neglect. *Curr Biol*. 2008:18: 1525–1529.

Weissenbacher A, Kasess C, Gerstl F, Lanzenberger R, Moser E, Windischberger C. Correlations and anticorrelations in resting-state functional connectivity MRI: a quantitative comparison of preprocessing strategies. *NeuroImage*. 2009:47:1408–1416.

Wilf M, Strappini F, Golan T, Hahamy A, Harel M, Malach R. Spontaneously emerging patterns in human visual cortex reflect responses to naturalistic sensory stimuli. *Cereb Cortex*. 2017:27: 750–763.

Wilf M, Serino A, Clarke S, Crottaz-Herbette S. Prism adaptation enhances decoupling between the default mode network and the attentional networks. *NeuroImage*. 2019:200:210–220.

Wilf M, Cheraka MC, Jeanneret M, Ott R, Perrin H, Crottaz-Herbette S, Serino A. Combined virtual reality and haptic robotics induce space and movement invariant sensorimotor adaptation. *Neuropsychologia*. 2021:150:107692.

Xu J, Branscheidt M, Schambra H, Steiner L, Widmer M, Diedrichsen J, Goldsmith J, Lindquist M, Kitago T, Luft AR. Rethinking interhemispheric imbalance as a target for stroke neurorehabilitation. *Ann Neurol*. 2019:85:502–513.

Yeo BT, Krienen FM, Sepulcre J, Sabuncu MR, Lashkari D, Hollinshead M, Roffman JL, Smoller JW, Zöllei L, Polimeni JR. The organization of the human cerebral cortex estimated by intrinsic functional connectivity. *J Neurophysiol*. 2011.

Yeshurun Y, Nguyen M, Hasson U. The default mode network: where the idiosyncratic self meets the shared social world. *Nat Rev Neurosci*. 2021:22:181–192.

Zhang YY, Brady M, Smith S. Segmentation of brain MR images through a hidden Markov random field model and the expectation-maximization algorithm. *IEEE Trans Med Imaging*. 2001:20:45–57.